

VL-RouterBench: A Benchmark for Vision–Language Model Routing

Zhehao Huang^{1,†} Baijiong Lin^{2,†,‡} Jingyuan Zhang¹ Jingying Wang¹
 Yuhang Liu¹ Ning Lu³ Tao Li¹ Xiaolin Huang^{1,✉}

¹Institute of Image Processing and Pattern Recognition, Shanghai Jiao Tong University

²The Hong Kong University of Science and Technology (Guangzhou)

³The Hong Kong University of Science and Technology

[†]Equal contribution [‡]Project lead [✉]Corresponding author

<https://github.com/K1nght/VL-RouterBench>

Abstract

Multi-model routing has evolved from an engineering technique into essential infrastructure, yet existing work lacks a systematic, reproducible benchmark for evaluating vision–language models (VLMs). We present **VL-RouterBench** to assess the overall capability of VLM routing systems systematically. The benchmark is grounded in raw inference and scoring logs from VLMs and constructs quality and cost matrices over sample–model pairs. In scale, VL-RouterBench covers 14 datasets across 3 task groups, totaling 30,540 samples, and includes 15 open-source models and 2 API models, yielding 519,180 sample–model pairs and a total input–output token volume of 34,494,977. The evaluation protocol jointly measures average accuracy, average cost, and throughput, and builds a ranking score to enable comparison across router configurations and cost budgets. On this benchmark, we evaluate 10 routing methods and baselines and observe a significant routability gain, while the best current routers still show a clear gap to the ideal Oracle, indicating considerable room for improvement in router architecture through finer visual cues and modeling of textual structure. We will open-source the complete data construction and evaluation toolchain to promote comparability, reproducibility, and practical deployment in multimodal routing research.

1. Introduction

In multi-model systems [1], the router has gradually evolved from an engineering optimization technique into critical infrastructure. As model families diversify and differ markedly in inference cost and capability, a single model can no longer ensure both performance and efficiency across all request types [2]. To address this, a router [3] performs dynamic

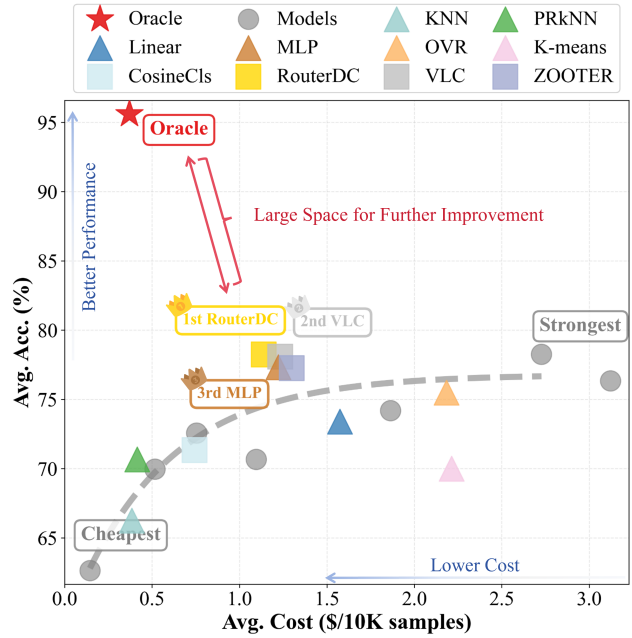


Figure 1. Overall performance comparison on VL-RouterBench. The x-axis and y-axis are Average Cost (Avg. Cost, \$/10K samples) and Average Accuracy (Avg. Acc., %), respectively. Gray dots denote the performance of single models at different costs, and “Strongest” and “Cheapest” mark the baselines that use only the strongest or the cheapest model. The gray dashed curve depicts the Pareto frontier fitted from these single-model points (only models near the frontier are shown for clarity). “1st RouterDC”, “2nd VLC”, and “3rd MLP” indicate the top three routers by Rank Score. Points closer to the upper left reflect a better accuracy–cost trade-off. The results show that even advanced routers still have a noticeable performance gap to the Oracle in the VLM routing setting.

model selection at the query level, enabling flexible trade-offs between quality and cost. The routing ecosystem built around this goal is expanding rapidly. In recent years research [4–7] has shown that selecting models at the task or sample level can substantially reduce average inference cost and end-to-end latency while largely preserving output quality, and on this basis more systematic evaluation practices

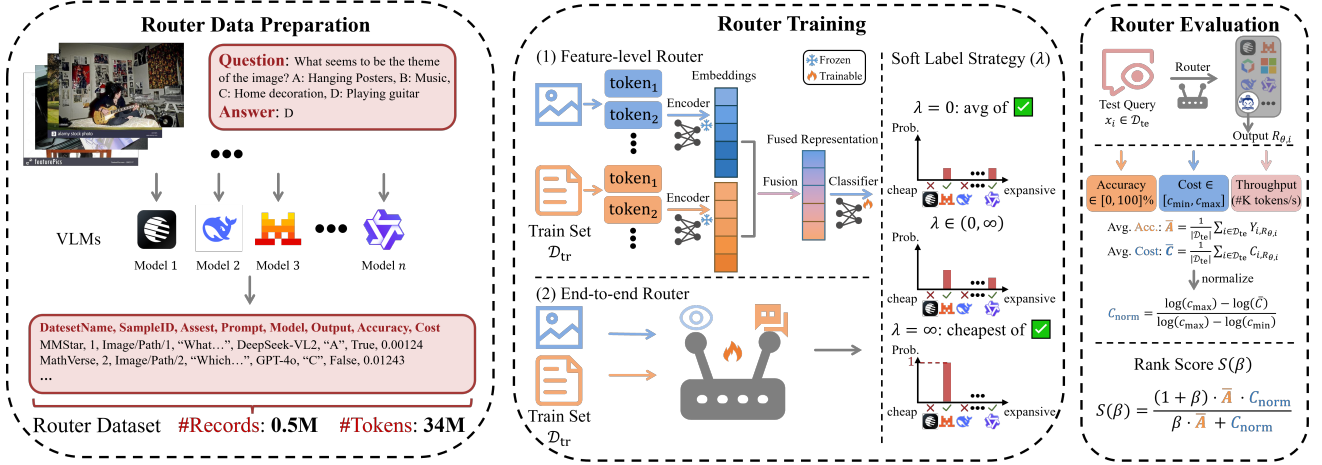


Figure 2. We propose VL-RouterBench to systematically assess the overall performance of vision-language model routing strategies. The three diagrams on the left, middle, and right represent Router Data Preparation (Sec. 3.2), Router Training (Sec. 3.3), and Router Evaluation (Sec. 3.4), respectively.

and open benchmarks [8–11] have emerged, advancing the routing paradigm from static rule based configuration to data driven learned router. At the same time, several mainstream commercial model families have embedded routing capabilities within unified product interfaces so that the underlying system can automatically schedule across models, for example the GPT-5¹ includes built in routing. Construction and evaluation of effective routers has become a shared need for engineering deployment and academic research.

Although routing research for large language models (LLMs) [12] is maturing, the vision–language model (VLM) [13] domain has long lacked a systematic and reproducible routing benchmark. Unlike LLM routing, VLM routing faces more challenges on multiple fronts. First, the task types supported by VLMs are highly diverse, including visual question answering (VQA) [14–18], visual reasoning [19–22], and chart OCR [23–26], and different tasks emphasize different aspects of model capability, which makes it more difficult to define what constitutes an “optimal” routing decision within a unified framework. Second, the mechanism of multimodal fusion remains an open problem [27]. Different VLMs vary substantially in modality interaction and semantic representation, which further increases the difficulty of router design and evaluation. Beyond these challenges, VLM routing also address issues introduced by the visual modality, such as the density of visual semantics [28] and cross-modal alignment [29]. These factors collectively distinguish VLM routing from LLM routing and constitute its unique difficulties. In view of these differences, we consider it both necessary and urgent to construct a VLM specific routing benchmark that can drive reproducible progress in the research and deployment of VLM routing systems.

We present **VL-RouterBench** to systematically evaluate the overall capability of VLM routing strategies. To ensure

reproducibility and comparability, we design a complete pipeline around router data preparation, router training, and router evaluation, as shown in **Fig. 2**. First, for data, we use raw inference and scoring logs from VLMs to construct quality and cost matrices. For each sample we retain the image path and textual instruction, the raw answers produced by each candidate model, correctness labels obtained by rule based evaluation as quality, and the counts of input and output tokens, from which we compute the sample level inference cost. In router training, we employ an adjustable soft label strategy that explicitly controls the trade-off between accuracy and cost, and we consider two routing architectural paradigms, namely feature-level routers and end-to-end routers. In router evaluation, we measure average accuracy, average cost, and throughput for each router on the test set, and we combine normalized cost and average accuracy by a harmonic mean to yield a single rank score, which allows researchers to compare different designs under a unified scale for accuracy and cost. Through large scale data collection, VL-RouterBench covers 14 datasets across three task groups with 30,540 samples, includes 15 open source models and 2 API models, and yields 519,180 sample–model pairs with a total input–output token volume of 34,494,977.

On VL-RouterBench, we systematically evaluate 10 routing methods and baselines, and further analyze the impact of different text and visual encoders, multimodal feature fusion methods, and multimodal backbones on routing performance, yielding conclusions that are consistent across settings and practically informative. First, we observe a significant routability reward. Under comparable or even lower cost, learned routing systems generally deliver stable gains in accuracy over any single model, which indicates that differences in difficulty and structure among multimodal samples can be effectively captured by lightweight routers. Second, text and visual embeddings followed by simple fu-

¹<https://openai.com/index/introducing-gpt-5>

sion schemes, such as normalized concatenation, suffices to support highly competitive routers and is consistently superior to counterparts that use only a single modality, which shows that multimodal input provides additional and fine grained discriminative signals for routing decisions. Finally, there remains a noticeable gap between the best current routing methods and the ideal Oracle, which suggests substantial potential for improving router architectures through finer visual cues and through modeling of layout and textual structure, as shown in [Fig. 1](#).

We will release the full pipeline to ensure that results are reproducible and extensible and that new models and data sources can be plugged in with minimal effort. Our main contributions are summarized below

1. We propose VL-RouterBench, a large scale benchmark for VLM routing systems that provides unified data and protocols for comparison of different routing methods.
2. We design a complete pipeline that covers data preparation, router training, and evaluation, and we introduce an adjustable soft label strategy that enables controllable trade-offs between accuracy and cost during training.
3. We conduct comprehensive comparisons and ablations of multiple routing methods on the benchmark, revealing the performance gap between current methods and the ideal Oracle, and offering guidance for future architectural design of VLM routers.

2. Related Work

2.1. Routing Systems

Multi-model routing systems [1] aim to dynamically select the most suitable model for each input to balance quality, cost, and throughput. Early methods [30], employed heuristic cascading strategies, invoking models in cost order to significantly reduce inference overhead. Later, systems [31] modeled routing as the "quality-cost-throughput" trilemma, validating the comprehensive advantages of learned routing in real-world scenarios. In terms of training methods, existing work can be divided into three categories: supervised learning based on performance logs [8], preference-based binary routing [32], and soft label training based on reward models [4, 33]. Although MoE models [34] also have routing mechanisms, they focus on conditional computations within a single network, which fundamentally differs from multi-model routing at the system level. Current research is mainly focused on LLM routers, and this paper extends the routing paradigm to vision–language scenarios, combining feature-level routing with end-to-end multimodal encoders to explore the impact of cross-modal representations on routing performance.

2.2. Vision-Language Models

The rapid development of general VLMs [13] provides a rich pool of candidate models for routing. BLIP-2 [35] provides a solution for cost-effective multimodal modeling by using a lightweight query Transformer, leveraging frozen image encoders and large frozen language models for vision-language pretraining. Building upon this, LLaVA [36] introduces visual instruction fine-tuning. InstructBLIP [37] systematically investigates cross-task instruction fine-tuning processes and module designs, reflecting the impact of training paradigms on generalization. Recently, the Qwen2.5-VL series [27] introduced a dynamic resolution mechanism, assigning adaptive numbers of visual tokens to each image, thereby clearly revealing the trade-off between visual fidelity and computation. In terms of evaluation, VLMEvalKit [38] integrates hundreds of proprietary and open-source large VLMs along with dozens of benchmark datasets under a unified generative protocol, enabling consistent cross-model comparison and large-scale log collection. Based on this ecosystem, our benchmark collects datasets from three major VLM task groups that are General, STEM, and Charts OCR, and pairs them with VLMs to provide standardized inference pathways for routing data.

2.3. Router Benchmarks

Routing evaluation for LLMs has gradually moved towards standardization in recent years. RouterBench [8] first proposed a systematic routing evaluation framework, providing theoretical analysis and comparisons across various routers based on a unified log format, offering a template and upper-bound estimation protocol for log-driven routing research. Subsequently, RouterEval [9] scaled up and systematically reported the model-level scaling-up phenomenon resulting from increased candidate pools and router capabilities meeting the mark, emphasizing the structural benefits of the routing paradigm relative to the single strongest model. To enhance horizontal comparability, RouterArena [11] built a routing evaluation dataset that covers a wide range of categories and difficulty levels, accompanied by multi-dimensional metrics including accuracy, cost ratio, optimal selection rate, latency, and robustness, along with an automated leaderboard update process, significantly lowering the barrier for new routing methods to be incorporated and continuously evaluated. All of the above benchmarks focus on text routing, whereas this paper is the first to build a unified evaluation benchmark tailored to the multimodal characteristics of VLMs, providing reproducible training and evaluation protocols.

3. VL-RouterBench Pipeline

3.1. Problem Formulation

We consider a routing framework for VLMs. Let the sample set be $\mathcal{D} = \{x_i = (I_i, T_i)\}_{i=1}^N$, where I_i denotes an image or a set of images and T_i denotes a textual instruction. The candidate multimodal model set is $\mathcal{M} = \{m_j\}_{j=1}^M$. For any sample i , the input is the multimodal pair $x_i = (I_i, T_i)$. A router parameterized by θ takes x_i as input and produces a decision distribution over models $\pi_\theta(\cdot | x_i)$, and during testing the model with the highest probability is selected as the routed model:

$$R_{\theta,i} = R(\theta, x_i) = \arg \max_{j \in \{1, \dots, M\}} \pi_\theta(m_j | x_i). \quad (1)$$

This formalization enables the router to adaptively assign each input, based on its visual and linguistic content, to the most suitable VLM while balancing performance and efficiency.

To systematically balance routing accuracy and cost, we model router training as a multi objective optimization problem. Let $Y_{i,j}$ and $C_{i,j}$ for each sample–model pair (i, j) denote a performance indicator (such as accuracy) and an inference cost (such as spending dollars). The training objective is

$$\min_{\theta} \underbrace{\mathbb{E}[-Y_{i,R_{\theta,i}}]}_{\text{performance risk}} + \lambda \underbrace{\mathbb{E}[C_{i,R_{\theta,i}}]}_{\text{expected cost}}, \quad (2)$$

where $\lambda \geq 0$ controls the penalty strength on cost. The objective jointly minimizes performance risk and expected cost to achieve a controllable balance of overall effectiveness, which provides a clear theoretical foundation for subsequent router training methods and supports systematic comparison and analysis of different routing strategies.

3.2. Router Data Preparation

We uniformly extract routing data from the inference and scoring artifacts of VLMEvalKit [38] to construct a standardized benchmark that ensures fairness and reproducibility of evaluation. To maintain consistency in quality assessment, we adopt a widely used setting in VLM evaluation where each sample prompt contains a single image and correctness can be verified by rule-based criteria, for example multiple choice and answer matching, thereby avoiding biases introduced by multi image inputs or subjective judgment. During data construction we do not consider task group labels of samples. Instead we organize the minimal data unit that records dataset name, sample index, image path, textual prompt, model name, model output, a boolean label for accuracy, and cost of input and output tokens. Using an automated verification procedure that compares model answers with the ground truth, we obtain a correctness label $Y_{i,j} \in \{0, 1\}$ for each sample–model pair (i, j)

and aggregate all records to form the global quality matrix $Y \in \mathbb{R}^{N \times M}$ for accuracy assessment. Cost is computed from token statistics in actual inference logs together with public model price sheets. Specifically, for sample i and model j the cost is

$$C_{i,j} = \#\text{tok_in}_{i,j} \cdot c_j^{\text{in}} + \#\text{tok_out}_{i,j} \cdot c_j^{\text{out}}, \quad (3)$$

where $\#\text{tok_in}_{i,j}$ and $\#\text{tok_out}_{i,j}$ denote the numbers of input and output tokens respectively, and c_j^{in} and c_j^{out} are the corresponding prices per million tokens for that model. This yields the cost matrix $C \in \mathbb{R}^{N \times M}$ for cost assessment. VL-RouterBench covers 14 datasets with 30,540 samples and involves 15 open source models and 2 API models, resulting in 519,180 complete inference records and a total token count of 34,494,977. The specific datasets and model choices are detailed in [Sec. 4.1](#) and [Sec. 4.2](#).

3.3. Router Training

We divide the entire routing dataset into a training set \mathcal{D}_{tr} , a validation set \mathcal{D}_{dev} , and a test set \mathcal{D}_{te} with the ratio $|\mathcal{D}_{\text{tr}}| : |\mathcal{D}_{\text{dev}}| : |\mathcal{D}_{\text{te}}| = 7 : 1 : 2$. This split is designed to ensure sufficient model training, reliable hyperparameter tuning, and independence of the final evaluation. The validation set is used to optimize the router hyperparameters under preset evaluation metrics so as to strike a reasonable balance between accuracy and cost.

Accuracy–Cost–Aware Soft Label Strategy. To introduce the trade-off between accuracy and cost into router training, we solve the Lagrangian optimization problem in [Eq. \(2\)](#) and obtain an analytic soft label target as

$$t_i^{(\lambda)}(j) = \frac{\mathbf{1}\{Y_{i,j} = 1\} \cdot g_\lambda(C_{i,j})}{\sum_{j:Y_{i,j}=1} g_\lambda(C_{i,j})}, \quad (4)$$

where $\mathbf{1}(\cdot)$ is the indicator function and $g_\lambda(\cdot)$ is a positive function that is monotonically decreasing in cost. Its proof is provided in [Appendix C](#). Intuitively, the router should place probability mass only on models that answer correctly and should prefer a correct model with lower cost. In practice, we adopt an exponential cost decay $g_\lambda(c) = \exp(-\lambda c)$, which yields a soft label target whose accuracy–cost trade-off is controlled by the hyperparameter $\lambda \geq 0$:

$$t_i^{(\lambda)}(j) = \frac{\mathbf{1}\{Y_{i,j} = 1\} \cdot \exp(-\lambda \cdot C_{i,j})}{\sum_{j:Y_{i,j}=1} \exp(-\lambda \cdot C_{i,j})}. \quad (5)$$

As shown in [Fig. 2](#), when $\lambda = 0$, cost is ignored and probability is distributed uniformly over all correct models, so the router focuses solely on accuracy. As $\lambda \rightarrow +\infty$, the objective strongly favors low cost, and the soft label degenerates to selecting only the cheapest correct model. For $0 < \lambda < +\infty$, the objective continuously balances accuracy

and cost. We then train the router parameters θ with the following soft label cross entropy loss:

$$\mathcal{L}_{\text{soft}}(\theta; \lambda) = \frac{1}{|\mathcal{D}_{\text{tr}}|} \sum_{i \in \mathcal{D}_{\text{tr}}} \text{KL}\left(t_i^{(\lambda)} \parallel \pi_{\theta}(\cdot \mid x_i)\right) \quad (6)$$

$$= \frac{1}{|\mathcal{D}_{\text{tr}}|} \sum_{i \in \mathcal{D}_{\text{tr}}} \sum_j t_i^{(\lambda)}(j) (-\log \pi_{\theta}(m_j \mid x_i)). \quad (7)$$

Regarding router architectures, we explore two paradigms. The first uses pretrained encoders to extract text and image features separately and then makes routing decisions with a classifier, as the feature-level router. The second processes multimodal inputs in an end-to-end manner and directly outputs the model selection, as the end-to-end router. Specific implementations are detailed in **Sec. 4.3** and Appendix G.

3.4. Router Evaluation & Metrics

To objectively compare different routers, we establish a multi-dimensional evaluation protocol centered on accuracy, cost, and efficiency. Let $R_{\theta,i}$ denote the final model decision made by the router for sample x_i . (1) **Average Accuracy (Avg. Acc.)** is

$$\bar{A} = \frac{1}{|\mathcal{D}_{\text{te}}|} \sum_{i \in \mathcal{D}_{\text{te}}} Y_{i,R_{\theta,i}}, \quad (8)$$

measured in percent and reflecting the overall correctness of routing decisions. (2) **Average Cost (Avg. Cost)** is

$$\bar{C} = \frac{1}{|\mathcal{D}_{\text{te}}|} \sum_{i \in \mathcal{D}_{\text{te}}} C_{i,R_{\theta,i}}, \quad (9)$$

by default presented as \$/10K samples, which quantifies the economic overhead during inference. (3) To promote comparability across router configurations, we follow [11] and introduce a multi-objective **Rank Score** that harmonically averages log normalized cost and accuracy. We first apply bounded normalization to cost. Given the full-sample cost range $[c_{\min}, c_{\max}]$, the normalized cost is

$$C_{\text{norm}} = 100 \times \frac{\log_2(c_{\max}) - \log_2(\bar{C})}{\log_2(c_{\max}) - \log_2(c_{\min})}, \quad (10)$$

which is multiplied by 100 to align with the percentage scale of Avg. Acc. We then combine accuracy and normalized cost using the harmonic mean as

$$S(\beta) = \frac{(1 + \beta) \cdot \bar{A} \cdot C_{\text{norm}}}{\beta \cdot \bar{A} + C_{\text{norm}}}, \quad (11)$$

where $\beta > 0$ controls the preference between quality and cost. By default we set $\beta = 0.1$ to prioritize accuracy. (4) **Throughput** measures system efficiency as the number of tokens processed per second in thousands of tokens per second (#K tokens/s), which evaluates the response efficiency

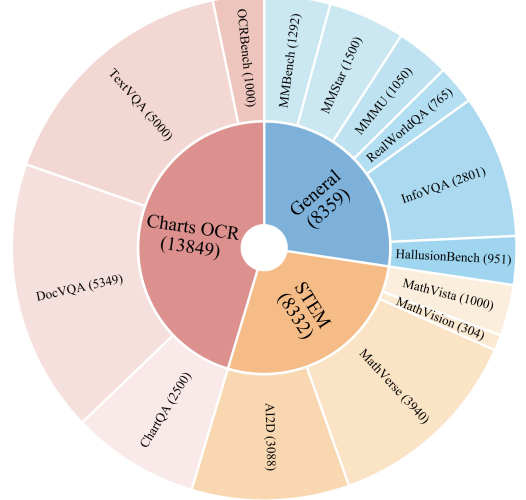


Figure 3. Dataset distribution in VL-RouterBench. The inner ring shows the three groups, and the outer ring lists the individual datasets. The numbers in parentheses indicate the number of samples contained in each entry.

of a deployed router system. (5) In addition to the quantitative metrics mentioned above, we further describe the overall trade-offs at different operating points by plotting accuracy–cost curves. For each given router, all its operating points in the accuracy–cost plane can be fitted into a curve, forming the **Pareto frontier**. Intuitively, the Pareto frontier closer to the upper left indicates that higher accuracy can be achieved at the same cost, or that lower cost can be achieved at the same accuracy. The detailed process of how to fit the Pareto frontier will be explained in Appendix D.

4. Benchmark Curation

4.1. Datasets

Our benchmark curates 14 datasets across three task groups, namely *General*, *STEM*, and *Charts OCR*, in order to induce sufficient routability differences and to cover diverse real application scenarios. The *General* group includes MM-Bench [14], MMStar [15], MMMU [16], RealWorldQA [17], InfoVQA [18], and HallusionBench [39], which together balance broad knowledge, evaluate cross domain understanding, assess infographic comprehension, and measure robustness. The *STEM* group covers MathVista [19], MathVision [20], MathVerse [21], and AI2D [22], focusing on structured visual cues and symbolic reasoning in mathematics and scientific diagrams. The *Charts and OCR/Document* group contains ChartQA [23], DocVQA [24], TextVQA [25], and OCRBench [26], and it systematically examines chart reading and integrated OCR capability. The data distribution is shown in **Fig. 3**, with detailed descriptions of the datasets available in Appendix E. This grouping and unified processing provide a solid foundation for routers to learn generalizable selection boundaries across multiple tasks.

Table 1. VLMs used in our benchmark, sorted by parameter count, with per-million-token prices for input and output. For the MoE model, m -A- n represents the total number of m B parameters in the model and the number of n B parameters activated during inference. All model prices are estimated based on the model size, compared with the prices on `Together.ai`.

Model	Params (B)	Input Price (\$/1M tokens)	Output Price (\$/1M tokens)
Janus-Pro-1B [40]	1.0	0.05	0.05
DeepSeek-VL2-Tiny [41]	27.0-A-1.0	0.05	0.05
SmolVLM2 [42]	2.2	0.06	0.06
Kimi-VL-A3B-Thinking-2506 [43]	16.0-A-2.8	0.20	0.25
Phi-3.5-Vision [44]	4.2	0.10	0.10
DeepSeek-VL2 [41]	27.0-A-4.5	0.35	0.50
Janus-Pro-7B [40]	7.0	0.18	0.25
MiMo-VL-7B-RL [45]	7.0	0.20	0.30
LLaVA-Next-Vicuna-7B [36]	7.0	0.20	0.20
Qianfan-VL-8B [46]	8.0	0.18	0.25
Pixtral-12B [47]	12.0	0.25	0.35
Gemma3-27B [48]	27.0	0.35	0.50
Qwen2.5-VL-32B-Instruct [27]	32.0	0.40	0.60
Qwen2.5-VL-72B-Instruct [27]	72.0	0.80	1.20
InternVL2.5-78B [49]	78.0	1.00	1.50
Gemini-Flash-2.5 [50]	-	0.30	2.40
GPT-4o [51]	-	2.50	10.00

4.2. Models

The core principle in building our model candidate pool is to ensure sufficient heterogeneity across models in terms of scale, architecture, and pricing, in order to realistically simulate the “quality–cost–latency” trilemma faced in actual deployment scenarios. To achieve this, we selected 15 open-source models and 2 API models, covering a parameter range from approximately 1B to 78B parameters, and incorporating a variety of mainstream vision encoding and modality alignment paradigms. The selected open-source models include: DeepSeek-VL2 [41], DeepSeek-VL2-Tiny [41], Gemma3-27B [48], InternVL2.5-78B [49], Janus-Pro-1B [40], Janus-Pro-7B [40], Kimi-VL-A3B-Thinking-2506 [43], LLaVA-Next-Vicuna-7B [36], MiMo-VL-7B-RL [45], Phi-3.5-Vision [44], Pixtral-12B [47], Qianfan-VL-8B [46], Qwen2.5-VL-32B-Instruct [27], Qwen2.5-VL-72B-Instruct [27], and SmolVLM2 [42]. The API models include GPT-4o [51] and Gemini-Flash-2.5 [50]. Model pricing is derived from the publicly available pricing policies of the AI cloud platform `Together.ai`², supplemented by estimates based on model size for those not listed. This approach ensures that cost metrics are both comparable and additive across all candidate models. A summary of model parameters and associated pricing is provided in **Tab. 1**, with comprehensive model descriptions available in Appendix F.

Note. The benchmark pipeline is highly scalable. Its streamlined architecture and modular inference framework enable the easy incorporation of newly released datasets and models. Through a unified feature extraction script, new data and models can be incrementally integrated into the quality–cost matrix, ensuring that this benchmark remains up-to-date

and in sync with the rapidly evolving ecosystem of vision-language models and cutting-edge routing research.

4.3. Routing Methods

Training-Free Baselines. We begin by introducing a set of training-free routing strategies to establish essential performance references for evaluating subsequent data-driven routers. Among them, **Oracle** establishes the theoretical performance upper bound for any router. It operates with perfect foresight: for each input sample, it selects the lowest-cost model that produces a correct response. If no model can answer the sample correctly, it falls back to the globally cheapest model to minimize cost. Formally, for a given sample x_i , we define the set of correct models as $\mathcal{S}_i \triangleq \{j \in \{1, \dots, M\} \mid Y_{i,j} = 1\}$. The Oracle routing decision is given by:

$$R^*(x_i) = \begin{cases} \arg \min_{j \in \mathcal{S}_i} C_{i,j}, & \text{if } \mathcal{S}_i \neq \emptyset \\ \arg \min_{j \in \{1, \dots, M\}} C_{i,j}, & \text{if } \mathcal{S}_i = \emptyset \end{cases}. \quad (12)$$

Strongest always selects the single model with the highest average accuracy on the entire training set \mathcal{D}_{tr} :

$$R^S(x_i) = \arg \max_{j \in \{1, \dots, M\}} \frac{1}{|\mathcal{D}_{\text{tr}}|} \sum_{i \in \mathcal{D}_{\text{tr}}} Y_{i,j}. \quad (13)$$

Conversely, **Cheapest** always selects the single model with the lowest average cost over the training set \mathcal{D}_{tr} :

$$R^C(x_i) = \arg \min_{j \in \{1, \dots, M\}} \frac{1}{|\mathcal{D}_{\text{tr}}|} \sum_{i \in \mathcal{D}_{\text{tr}}} C_{i,j}. \quad (14)$$

We now proceed to describe the two learning-based routing paradigms systematically studied in this benchmark.

Feature-level Routers. Feature-level routers extract embeddings $e_i^T = E^T(T_i)$, $e_i^I = E^I(I_i)$ from the frozen text encoder E^T and visual encoder E^I , respectively. The features from both modalities are then aggregated using a fusion function $F(\cdot, \cdot)$ to form a single feature $z_i = F(e_i^T, e_i^I)$. A lightweight classifier is then trained on this feature to predict the model selection distribution $\pi_\theta(\cdot \mid x_i) = \text{Cls}(z_i)$. We explore various classifier architectures, including **KNN** [52], **PRkNN** [53], **OVR** [54], **K-means** [52], **Linear** [52], and **MLP** [52], among others (see Appendix G for details). The training objective uses the previously defined accuracy–cost-aware soft label cross-entropy loss. The advantage of this paradigm lies in its excellent portability and training stability, which is well-suited for rapid iteration and feature-level ablation studies on large-scale offline logs, such as replacing visual encoders or adjusting fusion strategies, to better understand the contribution of multimodal representations to routability. Corresponding ablation results are presented and analyzed in **Sec. 5.3**.

²<https://www.together.ai/>

Table 2. Performance of Router Methods on VL-RouterBench. The best and second-best results except for Oracle are highlighted in **bold** and underlined, respectively. **Avg. Acc.** is average accuracy (%), **Avg. Cost** is average cost (\$/10K samples), **Rank** is sorted by Rank Score, and **Throughput** is measured in #K tokens/s.

Router	Avg. Acc. \uparrow	Avg. Cost \downarrow	Rank Score \uparrow	Rank \downarrow	Throughput \uparrow
<i>Training-free Baselines</i>					
Oracle	95.60	0.37	93.68	0	-
Strongest	<u>78.01</u>	2.72	68.88	8	-
Cheapest	62.43	0.14	64.63	11	-
<i>Feature-level Routers</i>					
KNN [52]	66.26	<u>0.38</u>	67.13	9	3.14
PRkNN [53]	70.68	0.41	71.09	5	2.73
OVR [54]	75.49	2.18	68.92	7	6.90
K-means [52]	70.01	2.21	64.62	12	31.43
Linear [52]	68.32 ± 7.45	1.32 ± 0.33	65.68 ± 5.69	10	150.74
MLP [52]	77.49 ± 0.56	1.13 ± 0.13	74.23 ± 0.22	3	<u>146.71</u>
<i>End-to-End Routers</i>					
CosineCls [4]	70.24 ± 0.62	0.61 ± 0.16	69.90 ± 0.34	6	7.58
RouterDC [4]	77.52 ± 1.04	1.04 ± 0.26	74.59 ± 1.05	1	6.31
ZOOTER [33]	74.65 ± 1.34	0.93 ± 0.15	72.58 ± 1.03	4	7.25
VLC [32]	78.09 ± 1.17	1.23 ± 0.03	74.33 ± 0.51	<u>2</u>	6.74

End-to-End Routers. directly learn the routing decision function from raw images and texts, fine-tuning the entire router network to adapt to specific task combinations. The goal is to capture finer-grained vision–language routing signals on high-difficulty samples. We refer to the design of BERT-Router [32] in traditional language model routing and explore four vision–language encoders as the backbone for routing: VisualBERT [55], UNITER [56], LXMERT [57], and ViLBERT [58], constructing a Vision–Language–Classification (VLC) Router and fine-tuning all parameters using the previously mentioned soft label cross-entropy loss. Additionally, we introduce various existing end-to-end routing training strategies, such as **CosineCls** [4], **RouterDC** [4], **ZOOTER** [33], etc., and evaluate their generalization capabilities in vision–language scenarios. Detailed descriptions of the vision–language encoder structures and routing training strategies can be found in Appendix G, with related architecture ablation studies presented in Sec. 5.3.

5. Experiments

5.1. Pilot Study between Oracle and Models

We first evaluate all candidate models along with the Oracle router on VL-RouterBench, and summarize the outcomes in Fig. 1 with full results provided in the Appendix I. The Oracle, representing the ideal routing strategy, achieves the highest accuracy at a very low cost, highlighting the significant potential of routing systems to enhance the cost-effectiveness of VLMs. Moreover, the substantial accuracy gap between the Oracle and any single model indicates considerable variation in model performance across different

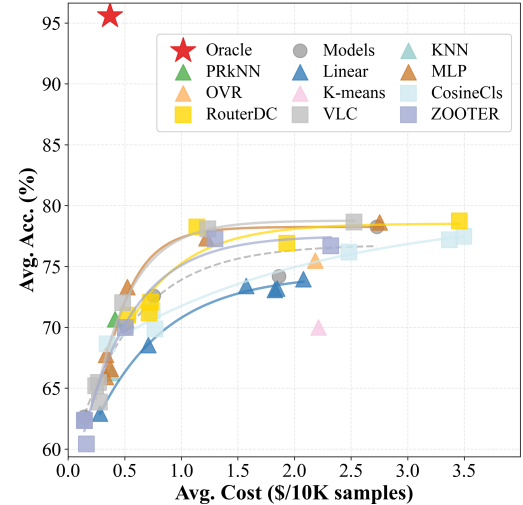


Figure 4. Performance in accuracy–cost plane. Gray dots represent baselines of individual models. Colored markers represent operating points of the same router under different λ , and curves are Pareto fronts fitted to these points. The closer to the upper left, the better the accuracy–cost trade-off.

samples, underscoring the existence of meaningful routing signals that can be exploited. It is also worth noting that certain open-source models deliver higher accuracy at lower costs compared to other candidates, emphasizing the challenge and opportunity in designing routers that effectively balance accuracy and cost in real-world settings.

Takeaway Message 5.1

The large Oracle–single-model performance gap indicates that routing potentially can substantially improve VLM cost-effectiveness compared with any single model.

5.2. Main Results on Router Methods

We evaluate all routing methods on VL-RouterBench after training with soft labels that reflect different accuracy–cost trade-offs. Specifically, we consider $\lambda = \{0, 10, 100, 1000, 10000, +\infty\}$, and the detailed training settings together with the hyperparameters of each method are provided in Appendix I. Tab. 2 reports, for each method, the results corresponding to its best Rank Score under the different trade-off settings. Most routing methods surpass the Strongest baseline, which is the single model with the highest accuracy, indicating that routing can indeed achieve high performance at lower cost than any single model. With a multimodal encoder architecture, the improved RouterDC attains the best Rank Score and reaches accuracy close to the strongest single model while using only one fifth of the cost. Fig. 4 presents the accuracy–cost Pareto frontiers of all methods to assess router performance across the global cost

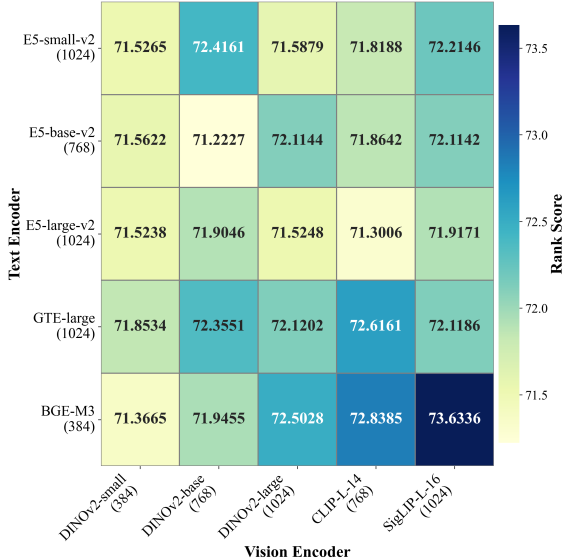


Figure 5. Performance comparison of different text and visual encoders paired on MLP with $\lambda = 100$. The brackets indicate the dimension of the encoder’s output embedding. Other settings are the same as in Table 2.

span. RouterDC and MLP significantly outperform the other routing methods and achieve similar Pareto optimal fronts. Nevertheless, there remains a substantial gap to the optimal Oracle, which suggests ample room for developing routers with better accuracy-cost trade-offs, while our benchmark provides a reproducible platform for such experimentation.

Takeaway Message 5.2

Most routers beat the best single-model baseline on the accuracy–cost trade-off, with **RouterDC** ranking highest. However, all methods still lag well behind the Oracle, showing substantial room to improve.

5.3. Ablation Study

Text and Visual Encoders. We conduct ablations on the encoders used to extract text and visual embeddings in the feature level router. Considering different embedding dimensions and architectures, we evaluate 5 text encoders, namely **E5-small/base/large-v2** [59], **GTE-large** [60], and **BGE-M3** [61], and 5 visual encoders, namely **DINOv2-small/base/large** [62], **CLIP-L-14** [29], and **SigLIP-L-16** [63]. We pair them in all combinations and train an MLP router. As shown in Fig. 5, increasing the dimensionality of text and visual embeddings effectively improves the router Rank Score. We adopt the best combination, BGE-M3 and SigLIP-L-16, as the embedding configuration for the feature level router.

Fusion Methods. We further examine fusion strategies after obtaining text and visual embeddings. We consider using

Table 3. Performance comparison of different fusion methods on MLP with $\lambda = 100$. The best and second-best results are highlighted in **bold** and underlined, respectively. Other settings are the same as in Table 2. Results are presented as mean and standard deviation across 5 independent trials.

Fusion Method	Avg. Acc. \uparrow	Avg. Cost \downarrow	Rank Score \uparrow	Throughput \uparrow
Only-Text	71.41 \pm 1.42	0.60 \pm 0.11	70.97 \pm 1.14	<u>147.21</u>
Only-Image	71.89 \pm 0.61	<u>0.50\pm0.13</u>	71.82 \pm 0.42	1550.65
Concat	72.35 \pm 0.93	0.63 \pm 0.06	71.70 \pm 1.03	146.71
Normalize-Concat	74.61 \pm 1.31	0.55 \pm 0.11	74.05\pm1.06	145.12
Weighted-Average	<u>74.78\pm1.02</u>	0.64 \pm 0.10	73.81 \pm 1.09	146.41
GMU [64]	81.81\pm1.71	3.32 \pm 0.09	69.12 \pm 1.44	141.25
MLB [65]	66.43 \pm 0.14	0.30\pm0.04	67.66 \pm 0.57	141.04

Table 4. Performance comparison of different backbones on VLC using $\lambda = 100$. The best and second-best results are highlighted in **bold** and underlined, respectively. Other settings are the same as in Table 2. Results are presented as mean and standard deviation across 5 independent trials.

Backbone	Image	Text	Avg. Acc. \uparrow	Avg. Cost \downarrow	Rank Score \uparrow	Throughput \uparrow
BERT [66]	\times	\checkmark	63.15 \pm 0.85	0.30\pm0.02	64.55 \pm 0.32	8.10
MobileNetV4 [67]	\checkmark	\times	<u>76.55\pm1.14</u>	3.92 \pm 0.45	63.33 \pm 0.72	8.93
VisualBERT [55]	\checkmark	\checkmark	70.54 \pm 1.12	0.43 \pm 0.12	<u>70.89\pm0.72</u>	6.32
UNITER [56]	\checkmark	\checkmark	67.69 \pm 1.10	0.39 \pm 0.06	68.43 \pm 0.72	6.44
LXMERT [57]	\checkmark	\checkmark	71.43 \pm 1.03	0.51 \pm 0.02	71.36\pm0.81	6.74
ViLBERT [58]	\checkmark	\checkmark	70.55 \pm 1.08	0.45 \pm 0.10	70.81 \pm 0.68	5.76

only the text embedding (**Only-Text**), only the image embedding (**Only-Image**), simple concatenation (**Concat**), normalization followed by concatenation (**Normalize-Concat**), and weighted fusion (**Weighted-Average**). We also include two methods that introduce additional projection parameters for fine tuning, **GMU** [64] and **MLB** [65]. Formal definitions of these methods are provided in Appendix G. Using the fused features, we train an MLP and report results in Tab. 3. As expected, Only-Text and Only-Image perform weaker because they use information from only one modality. GMU and MLB respectively emphasize accuracy and cost, but they are not competitive in terms of Rank Score. In contrast, Normalize-Concat yields the best accuracy and cost trade-off and is adopted as the default fusion method for all feature level routers. This indicates that there remains ample space to explore multimodal embedding fusion methods tailored for routing.

End-to-End Router Backbones. We next study the impact of the backbone in end-to-end routers. In addition to the 4 multimodal encoders that process both text and images in Sec. 4.3, we include two single modality baselines: **BERT** [66] from typical LLM router settings using only text, and **MobileNetV4** [67] from the vision modality using only images. The performance of different backbones is reported in Tab. 4. Because they consider only one modality, BERT and MobileNetV4 achieve markedly lower Rank Score than the four multimodal encoders. Among the multimodal encoders the results are very close, and we choose LXMERT, which attains the highest Rank Score, as the backbone for the end to end router. We expect that our benchmark will facilitate the development of multimodal encoder architec-

tures specifically designed for routing to further improve performance.

Takeaway Message 5.3

Higher-dimensional text and visual embeddings improve feature-level routing, with the **BGE-M3 + SigLIP-L-16** pairing performing best, and that simple multimodal fusion via **Normalize-Concat** delivers the strongest overall Rank Score. For end-to-end routers, multimodal backbones with **LXMERT** achieving the top performance among closely matched multimodal encoders.

5.4. Latency Profile

As the central component for model selection, the router must satisfy low latency and high throughput. The Throughput metric in **Tab. 2** shows that end to end router methods usually achieve a better accuracy and cost trade-off than feature level routers, yet their throughput is slightly lower due to the complexity of the backbone itself. For feature level routers the primary throughput bottleneck lies in the extraction of feature embeddings. Our benchmark offers a solid platform for studying lighter and higher throughput multimodal architectures specifically designed for routers.

Takeaway Message 5.4

End-to-end routers generally achieve better accuracy-cost trade-off than feature-level routers, but their throughput is slightly lower due to the complexity of the backbone itself.

6. Conclusion

In this paper, we introduced VL-RouterBench, a systematic and reproducible benchmark for routing in VLM systems. Grounded in raw inference and scoring logs from a pool of 15 open source models and 2 API models over 14 datasets for a total of 519,180 records, the benchmark constructs aligned sample-model quality and cost matrices that capture performance-cost trade-offs at scale and support a unified ranking score. On top of this construction, we defined an evaluation protocol that measures average accuracy, average cost, and throughput, and we evaluated 10 routing methods and baselines, including Oracle upper bounds and non-learned policies. The results reveal a clear routability reward: learned routers consistently outperform any single model at comparable or lower cost, while a sizable gap to the ideal Oracle frontier persists, especially in scenarios that require finer visual cues and more precise modeling of textual structure. We will open source the complete pipeline. Looking ahead, VL-RouterBench can be naturally extended to more complex

VLM settings, such as multiple image inputs or datasets with subjective or preference-based evaluation, thereby further broadening the application scope of routing and bringing benchmarks closer to real-world multimodal workflows.

7. Limitations

Here are some potential limitations of VL-RouterBench:

- **Single Image Input.** The current framework primarily considers single-image input scenarios for VLMs. This design limitation excludes more complex scenarios, such as multiple image inputs, which are relevant for many practical multimodal tasks like image captioning or image-based question answering that involve dynamic and large-scale images. Extending the benchmark to handle multi-image inputs could provide a more comprehensive evaluation of the routing system's capabilities
- **Binary Output Decision.** The routing decisions in the VL-RouterBench are based on a binary output model selection (correct or incorrect), while many real-world systems could benefit from more continuous score outputs. A more nuanced approach could involve probabilistic scoring, which would better capture the range of performance variation across models, improving the overall understanding of how well a model performs relative to another in a cost-sensitive manner.
- **Limited Evaluation of Cross-Modality.** Despite the extensive VLM dataset coverage across multiple domains, there is still a significant gap in evaluating cross-modal fusion mechanisms and multi-modal model capabilities. The benchmark primarily evaluates performance based on visual and textual data independently, but real-world applications often require complex fusion between multiple modalities, including audio, video, or even non-textual semantic information.
- **Robustness to Noisy or Imperfect Data.** VL-RouterBench is constructed from standardized logs with clean single-image prompts, and does not explicitly stress-test routers under noisy or imperfect inputs (e.g., typos, paraphrasing, or spurious visual artifacts). As a result, our evaluation primarily reflects routing performance under curated benchmark conditions and may overestimate robustness in real-world deployments where query quality is highly variable. Extending VL-RouterBench with perturbed or user-generated inputs and robustness-oriented metrics is an important direction for future work.

References

- [1] Jinliang Lu, Ziliang Pang, Min Xiao, Yaochen Zhu, Rui Xia, and Jiajun Zhang. Merge, ensemble, and cooperate! a survey on collaborative strategies in the era of large language models. *arXiv preprint arXiv:2407.06089*, 2024. 1, 3
- [2] Olaide N Oyelade, Hui Wang, and Karen Rafferty. A survey of adaptation of large language models to idea and hypothesis

generation: Downstream task adaptation, knowledge distillation approaches and challenges. *ACM Computing Surveys*, 2025. 1

[3] Yiqun Zhang, Hao Li, Jianhao Chen, Hangfan Zhang, Peng Ye, Lei Bai, and Shuyue Hu. Beyond gpt-5: Making llms cheaper and better via performance-efficiency optimized routing. *arXiv preprint arXiv:2508.12631*, 2025. 1

[4] Shuhao Chen, Weisen Jiang, Baijiong Lin, James T. Kwok, and Yu Zhang. Routerdc: Query-based router by dual contrastive learning for assembling large language models. In *NeurIPS*, 2024. 1, 3, 7, 5, 6

[5] Wei Song, Zhenya Huang, Cheng Cheng, Weibo Gao, Bihai Xu, Guanhao Zhao, Fei Wang, and Runze Wu. Irt-router: Effective and interpretable multi-llm routing via item response theory. In *ACL (1)*, pages 15629–15644. Association for Computational Linguistics, 2025.

[6] Zhou Chen, Zhiqiang Wei, Yuqi Bai, Xue Xiong, and Jianmin Wu. Tagrouter: Learning route to llms through tags for open-domain text generation tasks. In *ACL (Findings)*, pages 21539–21564. Association for Computational Linguistics, 2025.

[7] Tao Feng, Yanzhen Shen, and Jiaxuan You. Graphrouter: A graph-based router for LLM selections. In *ICLR*. OpenReview.net, 2025. 1

[8] Qitian Jason Hu, Jacob Bieker, Xiuyu Li, Nan Jiang, Benjamin Keigwin, Gaurav Ranganath, Kurt Keutzer, and Shriyash Kaustubh Upadhyay. Routerbench: A benchmark for multi-llm routing system, 2024. 2, 3

[9] Zhongzhan Huang, Guoming Ling, Yupei Lin, Yandong Chen, Shanshan Zhong, Hefeng Wu, and Liang Lin. Routereval: A comprehensive benchmark for routing llms to explore model-level scaling up in llms, 2025. 3

[10] Tao Feng, Haozhen Zhang, Zijie Lei, Pengrui Han, Mostofa Patwary, Mohammad Shoeybi, Bryan Catanzaro, and Jiaxuan You. Fusionfactory: Fusing llm capabilities with multi-llm log data, 2025.

[11] Yifan Lu, Rixin Liu, Jiayi Yuan, Xingqi Cui, Shenrun Zhang, Hongyi Liu, and Jiarong Xing. Routerarena: An open platform for comprehensive comparison of llm routers, 2025. 2, 3, 5

[12] Andrea Matarazzo and Riccardo Torlone. A survey on large language models with some insights on their capabilities and limitations. *arXiv preprint arXiv:2501.04040*, 2025. 2

[13] Zongxia Li, Xiyang Wu, Hongyang Du, Fuxiao Liu, Huy Nghiem, and Guanyao Shi. A survey of state of the art large vision language models: Alignment, benchmark, evaluations and challenges. *arXiv preprint arXiv:2501.02189*, 2025. 2, 3

[14] Yuan Liu, Haodong Duan, Yuanhan Zhang, Bo Li, Songyang Zhang, Wangbo Zhao, Yike Yuan, Jiaqi Wang, Conghui He, Ziwei Liu, et al. Mmbench: Is your multi-modal model an all-around player? In *European conference on computer vision*, pages 216–233. Springer, 2024. 2, 5, 3

[15] Lin Chen, Jinsong Li, Xiaoyi Dong, Pan Zhang, Yuhang Zang, Zehui Chen, Haodong Duan, Jiaqi Wang, Yu Qiao, Dahua Lin, et al. Are we on the right way for evaluating large vision-language models? *Advances in Neural Information Processing Systems*, 37:27056–27087, 2024. 5, 3

[16] Xiang Yue, Yuansheng Ni, Kai Zhang, Tianyu Zheng, Ruqi Liu, Ge Zhang, Samuel Stevens, Dongfu Jiang, Weiming Ren, Yuxuan Sun, et al. Mmmu: A massive multi-discipline multi-modal understanding and reasoning benchmark for expert agi. In *Proceedings of the IEEE/CVF Conference on Computer Vision and Pattern Recognition*, pages 9556–9567, 2024. 5, 3

[17] xAI. Grok-1.5 vision preview, 2024. 5, 3

[18] Minesh Mathew, Viraj Bagal, Rubén Tito, Dimosthenis Karatzas, Ernest Valveny, and CV Jawahar. Infographicvqa. In *Proceedings of the IEEE/CVF Winter Conference on Applications of Computer Vision*, pages 1697–1706, 2022. 2, 5, 3

[19] Pan Lu, Hritik Bansal, Tony Xia, Jiacheng Liu, Chunyuan Li, Hannaneh Hajishirzi, Hao Cheng, Kai-Wei Chang, Michel Galley, and Jianfeng Gao. Mathvista: Evaluating mathematical reasoning of foundation models in visual contexts. *arXiv preprint arXiv:2310.02255*, 2023. 2, 5, 3

[20] Ke Wang, Junting Pan, Weikang Shi, Zimu Lu, Houxing Ren, Aojun Zhou, Mingjie Zhan, and Hongsheng Li. Measuring multimodal mathematical reasoning with math-vision dataset. *Advances in Neural Information Processing Systems*, 37:95095–95169, 2024. 5, 3

[21] Renrui Zhang, Dongzhi Jiang, Yichi Zhang, Haokun Lin, Ziyu Guo, Pengshuo Qiu, Aojun Zhou, Pan Lu, Kai-Wei Chang, Yu Qiao, et al. Mathverse: Does your multi-modal llm truly see the diagrams in visual math problems? In *European Conference on Computer Vision*, pages 169–186. Springer, 2024. 5, 3

[22] Aniruddha Kembhavi, Mike Salvato, Eric Kolve, Minjoon Seo, Hannaneh Hajishirzi, and Ali Farhadi. A diagram is worth a dozen images. In *European conference on computer vision*, pages 235–251. Springer, 2016. 2, 5, 3

[23] Ahmed Masry, Xuan Long Do, Jia Qing Tan, Shafiq Joty, and Enamul Hoque. Chartqa: A benchmark for question answering about charts with visual and logical reasoning. In *Findings of the association for computational linguistics: ACL 2022*, pages 2263–2279, 2022. 2, 5, 4

[24] Minesh Mathew, Dimosthenis Karatzas, and CV Jawahar. Docvqa: A dataset for vqa on document images. In *Proceedings of the IEEE/CVF winter conference on applications of computer vision*, pages 2200–2209, 2021. 5, 4

[25] Amanpreet Singh, Vivek Natarajan, Meet Shah, Yu Jiang, Xinlei Chen, Dhruv Batra, Devi Parikh, and Marcus Rohrbach. Towards vqa models that can read. In *Proceedings of the IEEE/CVF conference on computer vision and pattern recognition*, pages 8317–8326, 2019. 5, 3

[26] Yuliang Liu, Zhang Li, Mingxin Huang, Biao Yang, Wenwen Yu, Chunyuan Li, Xu-Cheng Yin, Cheng-Lin Liu, Lianwen Jin, and Xiang Bai. Ocrbench: on the hidden mystery of ocr in large multimodal models. *Science China Information Sciences*, 67(12):220102, 2024. 2, 5, 4

[27] Shuai Bai, Keqin Chen, Xuejing Liu, Jialin Wang, Wenbin Ge, Sibo Song, Kai Dang, Peng Wang, Shijie Wang, Jun Tang, et al. Qwen2.5-vl technical report. *arXiv preprint arXiv:2502.13923*, 2025. 2, 3, 6, 5

[28] Luca Rossetto, Cristina Sarasua, and Abraham Bernstein. Estimating the semantic density of visual media. In *ACM Multimedia*, pages 4601–4609. ACM, 2024. 2

[29] Alec Radford, Jong Wook Kim, Chris Hallacy, Aditya Ramesh, Gabriel Goh, Sandhini Agarwal, Girish Sastry,

Amanda Askell, Pamela Mishkin, Jack Clark, Gretchen Krueger, and Ilya Sutskever. Learning transferable visual models from natural language supervision. In *ICML*, volume 139 of *Proceedings of Machine Learning Research*, pages 8748–8763. PMLR, 2021. 2, 8

[30] Lingjiao Chen, Matei Zaharia, and James Zou. Frugalgpt: How to use large language models while reducing cost and improving performance. *arXiv preprint arXiv:2305.05176*, 2023. 3

[31] Dimitris Stripelis, Zhaozhuo Xu, Zijian Hu, Alay Dilipbhai Shah, Han Jin, Yuhang Yao, Jipeng Zhang, Tong Zhang, Salman Avestimehr, and Chaoyang He. Tensoropera router: A multi-model router for efficient LLM inference. In *EMNLP (Industry Track)*, pages 452–462. Association for Computational Linguistics, 2024. 3

[32] Isaac Ong, Amjad Almahairi, Vincent Wu, Wei-Lin Chiang, Tianhao Wu, Joseph E. Gonzalez, M. Waleed Kadous, and Ion Stoica. Routellm: Learning to route llms from preference data. In *ICLR*. OpenReview.net, 2025. 3, 7

[33] Keming Lu, Hongyi Yuan, Runji Lin, Junyang Lin, Zheng Yuan, Chang Zhou, and Jingren Zhou. Routing to the expert: Efficient reward-guided ensemble of large language models. In *NAACL-HLT*, pages 1964–1974. Association for Computational Linguistics, 2024. 3, 7, 6

[34] Weilin Cai, Juyong Jiang, Fan Wang, Jing Tang, Sunghun Kim, and Jiayi Huang. A survey on mixture of experts in large language models. *IEEE Transactions on Knowledge and Data Engineering*, 2025. 3

[35] Junnan Li, Dongxu Li, Silvio Savarese, and Steven C. H. Hoi. BLIP-2: bootstrapping language-image pre-training with frozen image encoders and large language models. In *ICML*, volume 202 of *Proceedings of Machine Learning Research*, pages 19730–19742. PMLR, 2023. 3

[36] Bo Li, Hao Zhang, Kaichen Zhang, Dong Guo, Yuanhan Zhang, Renrui Zhang, Feng Li, Ziwei Liu, and Chunyuan Li. Llava-next: What else influences visual instruction tuning beyond data?, May 2024. 3, 6, 4

[37] Wenliang Dai, Junnan Li, Dongxu Li, Anthony Meng Huat Tiong, Junqi Zhao, Weisheng Wang, Boyang Li, Pascale Fung, and Steven C. H. Hoi. Instructblip: Towards general-purpose vision-language models with instruction tuning. In *NeurIPS*, 2023. 3

[38] Haodong Duan, Junming Yang, Yuxuan Qiao, Xinyu Fang, Lin Chen, Yuan Liu, Xiaoyi Dong, Yuhang Zang, Pan Zhang, Jiaqi Wang, Dahua Lin, and Kai Chen. Vlmevalkit: An open-source toolkit for evaluating large multi-modality models. In *ACM Multimedia*, pages 11198–11201. ACM, 2024. 3, 4

[39] Tianrui Guan, Fuxiao Liu, Xiyang Wu, Ruiqi Xian, Zongxia Li, Xiaoyu Liu, Xijun Wang, Lichang Chen, Furong Huang, Yaser Yacoob, et al. Hallusionbench: an advanced diagnostic suite for entangled language hallucination and visual illusion in large vision-language models. In *Proceedings of the IEEE/CVF Conference on Computer Vision and Pattern Recognition*, pages 14375–14385, 2024. 5, 3

[40] Xiaokang Chen, Zhiyu Wu, Xingchao Liu, Zizheng Pan, Wen Liu, Zhenda Xie, Xingkai Yu, and Chong Ruan. Janus-pro: Unified multimodal understanding and generation with data and model scaling. *arXiv preprint arXiv:2501.17811*, 2025. 6, 4

[41] Zhiyu Wu, Xiaokang Chen, Zizheng Pan, Xingchao Liu, Wen Liu, Damai Dai, Huazuo Gao, Yiyang Ma, Chengyue Wu, Bingxuan Wang, et al. Deepseek-vl2: Mixture-of-experts vision-language models for advanced multimodal understanding. *arXiv preprint arXiv:2412.10302*, 2024. 6, 4

[42] Andrés Marafioti, Orr Zohar, Miquel Farré, Merve Noyan, Elie Bakouch, Pedro Cuenca, Cyril Zakka, Loubna Ben Allal, Anton Lozhkov, Nouamane Tazi, et al. Smolvlm: Redefining small and efficient multimodal models. *arXiv preprint arXiv:2504.05299*, 2025. 6, 5

[43] Kimi Team, Angang Du, Bohong Yin, Bowei Xing, Bowen Qu, Bowen Wang, Cheng Chen, Chenlin Zhang, Chenzhuang Du, Chu Wei, et al. Kimi-vl technical report. *arXiv preprint arXiv:2504.07491*, 2025. 6, 4

[44] Marah Abdin, Jyoti Aneja, Hany Awadalla, Ahmed Awadallah, Ammar Ahmad Awan, Nguyen Bach, Amit Bahree, Arash Bakhtiari, Jianmin Bao, Harkirat Behl, Alon Benhaim, Misha Bilenko, Johan Bjorck, Sébastien Bubeck, Martin Cai, Qin Cai, Vishrav Chaudhary, Dong Chen, Dongdong Chen, Weizhu Chen, Yen-Chun Chen, Yi-Ling Chen, Hao Cheng, Parul Chopra, Xiyang Dai, Matthew Dixon, Ronen Eldan, Victor Fragoso, Jianfeng Gao, Mei Gao, Min Gao, Amit Garg, Allie Del Giorno, Abhishek Goswami, Suriya Gunasekar, Emmanuel Haider, Junheng Hao, Russell J. Hewett, Wenxiang Hu, Jamie Huynh, Dan Iter, Sam Ade Jacobs, Mojan Javaheripi, Xin Jin, Nikos Karampatziakis, Piero Kauffmann, Mahoud Khademi, Dongwoo Kim, Young Jin Kim, Lev Kurilenko, James R. Lee, Yin Tat Lee, Yuanzhi Li, Yunsheng Li, Chen Liang, Lars Liden, Xihui Lin, Zeqi Lin, Ce Liu, Liyuan Liu, Mengchen Liu, Weishung Liu, Xiaodong Liu, Chong Luo, Piyush Madan, Ali Mahmoudzadeh, David Majercak, Matt Mazzola, Caio César Teodoro Mendes, Arindam Mitra, Hardik Modi, Anh Nguyen, Brandon Norick, Barun Patra, Daniel Perez-Becker, Thomas Portet, Reid Pryzant, Heyang Qin, Marko Radmilac, Liliang Ren, Gustavo de Rosa, Corby Rosset, Sambudha Roy, Olatunji Ruwase, Olli Saarikivi, Amin Saied, Adil Salim, Michael Santacroce, Shital Shah, Ning Shang, Hiteshi Sharma, Yelong Shen, Swadheen Shukla, Xia Song, Masahiro Tanaka, Andrea Tupini, Praneetha Vadadamanu, Chunyu Wang, Guanhua Wang, Lijuan Wang, Shuhang Wang, Xin Wang, Yu Wang, Rachel Ward, Wen Wen, Philipp Witte, Haiping Wu, Xiaoxia Wu, Michael Wyatt, Bin Xiao, Can Xu, Jiahang Xu, Weijian Xu, Jilong Xue, Sonali Yadav, Fan Yang, Jianwei Yang, Yifan Yang, Ziyi Yang, Donghan Yu, Lu Yuan, Chenruidong Zhang, Cyril Zhang, Jianwen Zhang, Li Lyra Zhang, Yi Zhang, Yue Zhang, Yunan Zhang, and Xiren Zhou. Phi-3 technical report: A highly capable language model locally on your phone, 2024. 6, 4

[45] Xiaomi LLM-Core Team Zihao Yue, Zhenrui Lin, Yi-Hao Song, Weikun Wang, Shu-Qin Ren, Shuhao Gu, Shicheng Li, Peidian Li, Liang Zhao, Lei Li, Kainan Bao, Hao Tian, Hailin Zhang, Gang Wang, Dawei Zhu, Cici, Chenhong He, Bowen Ye, Bowen Shen, Zihan Zhang, Zi-Ang Jiang, Zhipian Zheng, Zhichao Song, Zhen Luo, Yue Yu, Yudong Wang, Yu Tian, Yu Tu, Yihan Yan, Yi Huang, Xu Wang, Xin dan Xu, Xin Ran Song, Xing Zhang, Xing Yong, Xin Zhang, Xia

Deng, Wenyu Yang, Wenhan Ma, Weiwei Lv, Weiji Zhuang, Wei Liu, Sirui Deng, Shuo Liu, Shimao Chen, Shi liang Yu, Shao yang Liu, Shan yong Wang, Rui Ma, Qiantong Wang, Peng Wang, Nuo Chen, Menghang Zhu, Kang Zhou, Kang Zhou, Kai Fang, Jun-Miao Shi, Jinhao Dong, Jiebao Xiao, Jiaming Xu, Huaiqiu Liu, Hongsheng Xu, Hengxu Qu, Hao-Song Zhao, Hanglong Lv, Guoan Wang, Duo Zhang, Dong Zhang, Di Zhang, Chong-Yi Ma, Chang Liu, Can Cai, and Bing Xia. Mimo-vl technical report. *ArXiv*, abs/2506.03569, 2025. [6](#), [4](#)

[46] Daxiang Dong, Mingming Zheng, Dong Xu, Bairong Zhuang, Wenyu Zhang, Chunhua Luo, Haoran Wang, Zijian Zhao, Jie Li, Yuxuan Li, et al. Qianfan-vl: Domain-enhanced universal vision-language models. *arXiv preprint arXiv:2509.18189*, 2025. [6](#), [4](#)

[47] Pravesh Agrawal, Szymon Antoniak, Emma Bou Hanna, Baptiste Bout, Devendra Chaplot, Jessica Chudnovsky, Diogo Costa, Baudouin De Monicault, Saurabh Garg, Theophile Gervet, et al. Pixtral 12b. *arXiv preprint arXiv:2410.07073*, 2024. [6](#), [4](#)

[48] Gemma Team, Aishwarya Kamath, Johan Ferret, Shreya Pathak, Nino Vieillard, Ramona Merhej, Sarah Perrin, Tatiana Matejovicova, Alexandre Ramé, Morgane Rivière, et al. Gemma 3 technical report. *arXiv preprint arXiv:2503.19786*, 2025. [6](#), [4](#)

[49] Zhe Chen, Weiyun Wang, Yue Cao, Yangzhou Liu, Zhang-wei Gao, Erfei Cui, Jinguo Zhu, Shenglong Ye, Hao Tian, Zhaoyang Liu, et al. Expanding performance boundaries of open-source multimodal models with model, data, and test-time scaling. *arXiv preprint arXiv:2412.05271*, 2024. [6](#), [4](#)

[50] Gheorghe Comanici, Eric Bieber, Mike Schaeckermann, Ice Pasupat, Noveen Sachdeva, Inderjit Dhillon, Marcel Blistein, Ori Ram, Dan Zhang, Evan Rosen, et al. Gemini 2.5: Pushing the frontier with advanced reasoning, multimodality, long context, and next generation agentic capabilities. *arXiv preprint arXiv:2507.06261*, 2025. [6](#), [5](#)

[51] Aaron Hurst, Adam Lerer, Adam P Goucher, Adam Perelman, Aditya Ramesh, Aidan Clark, AJ Ostrow, Akila Welihinda, Alan Hayes, Alec Radford, et al. Gpt-4o system card. *arXiv preprint arXiv:2410.21276*, 2024. [6](#), [5](#)

[52] Tal Shnitzer, Anthony Ou, Mírian Silva, Kate Soule, Yuekai Sun, Justin Solomon, Neil Thompson, and Mikhail Yurochkin. Large language model routing with benchmark datasets. *arXiv preprint arXiv:2309.15789*, 2023. [6](#), [7](#), [5](#)

[53] Yandong Zheng, Hui Zhu, Rongxing Lu, Yunguo Guan, Song-nian Zhang, Fengwei Wang, Jun Shao, and Hui Li. Efficient and privacy-preserving aggregated reverse knn query over crowd-sensed data. *IEEE Trans. Inf. Forensics Secur.*, 18:4285–4299, 2023. [6](#), [7](#), [5](#)

[54] Ryan M. Rifkin and Aldebaro Klautau. In defense of one-vs-all classification. *J. Mach. Learn. Res.*, 5:101–141, 2004. [6](#), [7](#), [5](#)

[55] Liunian Harold Li, Mark Yatskar, Da Yin, Cho-Jui Hsieh, and Kai-Wei Chang. Visualbert: A simple and performant baseline for vision and language. *arXiv preprint arXiv:1908.03557*, 2019. [7](#), [8](#), [6](#)

[56] Yen-Chun Chen, Linjie Li, Licheng Yu, Ahmed El Kholy, Faisal Ahmed, Zhe Gan, Yu Cheng, and Jingjing Liu. UNITER: universal image-text representation learning. In *ECCV (30)*, volume 12375 of *Lecture Notes in Computer Science*, pages 104–120. Springer, 2020. [7](#), [8](#), [6](#)

[57] Hao Tan and Mohit Bansal. LXMERT: learning cross-modality encoder representations from transformers. In *EMNLP/IJCNLP (1)*, pages 5099–5110. Association for Computational Linguistics, 2019. [7](#), [8](#), [6](#)

[58] Jiasen Lu, Dhruv Batra, Devi Parikh, and Stefan Lee. Vilbert: Pretraining task-agnostic visiolinguistic representations for vision-and-language tasks. In *NeurIPS*, pages 13–23, 2019. [7](#), [8](#), [6](#)

[59] Liang Wang, Nan Yang, Xiaolong Huang, Binxing Jiao, Lin-jun Yang, Dixin Jiang, Rangan Majumder, and Furu Wei. Text embeddings by weakly-supervised contrastive pre-training. *arXiv preprint arXiv:2212.03533*, 2022. [8](#)

[60] Zehan Li, Xin Zhang, Yanzhao Zhang, Dingkun Long, Pengjun Xie, and Meishan Zhang. Towards general text embeddings with multi-stage contrastive learning. *arXiv preprint arXiv:2308.03281*, 2023. [8](#)

[61] Jianlv Chen, Shitao Xiao, Peitian Zhang, Kun Luo, Defu Lian, and Zheng Liu. Bge m3-embedding: Multi-lingual, multi-functionality, multi-granularity text embeddings through self-knowledge distillation, 2024. [8](#)

[62] Maxime Oquab, Timothée Darcet, Théo Moutakanni, Huy V. Vo, Marc Szafraniec, Vasil Khalidov, Pierre Fernandez, Daniel Haziza, Francisco Massa, Alaaeldin El-Nouby, Mido Assran, Nicolas Ballas, Wojciech Galuba, Russell Howes, Po-Yao Huang, Shang-Wen Li, Ishan Misra, Michael Rabat, Vasu Sharma, Gabriel Synnaeve, Hu Xu, Hervé Jégou, Julien Mairal, Patrick Labatut, Armand Joulin, and Piotr Bojanowski. Dinov2: Learning robust visual features without supervision. *Trans. Mach. Learn. Res.*, 2024, 2024. [8](#)

[63] Xiaohua Zhai, Basil Mustafa, Alexander Kolesnikov, and Lucas Beyer. Sigmoid loss for language image pre-training. In *ICCV*, pages 11941–11952. IEEE, 2023. [8](#)

[64] John Arevalo, Thamar Solorio, Manuel Montes-y Gómez, and Fabio A González. Gated multimodal units for information fusion. *arXiv preprint arXiv:1702.01992*, 2017. [8](#), [6](#)

[65] Kankana Roy. Multimodal score fusion with sparse low-rank bilinear pooling for egocentric hand action recognition. *ACM Trans. Multim. Comput. Commun. Appl.*, 20(7):227:1–227:22, 2024. [8](#), [6](#)

[66] Jacob Devlin, Ming-Wei Chang, Kenton Lee, and Kristina Toutanova. BERT: pre-training of deep bidirectional transformers for language understanding. In *NAACL-HLT (1)*, pages 4171–4186. Association for Computational Linguistics, 2019. [8](#), [6](#)

[67] Danfeng Qin, Chas Leichner, Manolis Delakis, Marco Fornoni, Shixin Luo, Fan Yang, Weijun Wang, Colby R. Banbury, Chengxi Ye, Berkin Akin, Vaibhav Aggarwal, Tenghui Zhu, Daniele Moro, and Andrew G. Howard. Mobilenetv4: Universal models for the mobile ecosystem. In *ECCV (40)*, volume 15098 of *Lecture Notes in Computer Science*, pages 78–96. Springer, 2024. [8](#), [6](#)

VL-RouterBench: A Benchmark for Vision–Language Model Routing

Supplementary Material

A. Implications

VL-RouterBench provides not only a standardized benchmark for VLM routing, but also several broader implications for the design of multimodal systems, routing algorithms, and future evaluation practice.

- **Implications for multimodal representation and router architecture.** Our results show that lightweight multimodal representations (frozen text and image encoders with simple fusion) already support competitive feature-level routers, while end-to-end VLC-style encoders further improve Rank Score at a modest throughput cost. This suggests that routing primarily relies on *coarse but discriminative* multimodal features, motivating router-specific encoders optimized for predicting which downstream model will succeed rather than for full answer generation.
- **Cost-aware training as a general recipe.** By casting routing as a multi-objective optimization over performance and cost and deriving a soft-label target that concentrates probability on correct yet cheaper models, VL-RouterBench provides a generic recipe for cost-aware training. The same Lagrangian-based construction can be reused in other multi-LLM or multi-VLM settings such as tool selection, CoT depth selection, or dynamic resolution control.
- **Towards more realistic multimodal routing workloads.** Built from large-scale VLMEvalKit logs over 14 datasets and 17 models, VL-RouterBench already approximates a realistic mixture of General, STEM, and Charts/OCR workloads, enabling offline prototyping of routing policies and their quality–cost–throughput trade-offs. It also encourages *workload-aware routing*, where router designs and model pools are tailored to domain-specific mixtures of difficulty and modality structure.
- **Bridging LLM routing benchmarks and multimodal routing.** VL-RouterBench extends existing LLM routing benchmarks into the multimodal regime, showing that ideas such as log-based evaluation, deferral curves, optimality analysis, and model-pool scaling transfer naturally but face new challenges from visual tokens and cross-modal alignment. This offers a shared conceptual and tooling foundation for unified routing frameworks across text-only LLMs, VLMs, and future audio or video models.

B. Ethics Statement

- **Data Sources and Privacy.** All data in VL-RouterBench originates from established vision-language benchmarks and the VLMEvalKit framework. We use only publicly available images, texts, and annotations under their respective licenses. The benchmark involves no human data

collection, no user interaction, and no attempt to identify individuals. To our knowledge, the underlying datasets contain no personally identifiable information.

- **Methodological Scope.** Our routing approach operates purely at the model selection level and does not modify model internals or training data. While the benchmark itself involves no real-world deployment, we note that selected models may inherit and potentially amplify biases, stereotypes, or harmful behaviors present in their original training corpora.
- **Use Restrictions.** We explicitly prohibit using VL-RouterBench or its components for optimizing routing in harmful applications, including discrimination, misinformation, or surveillance systems. Any practical deployment should incorporate independent safety mechanisms and domain-specific guardrails.

C. Proof of the Soft Label Strategy

We consider the routing framework for VLMs described in Sec. 3.1. Let the dataset be $\mathcal{D} = \{x_i = (I_i, T_i)\}_{i=1}^N$ and the candidate model set be $\mathcal{M} = \{m_j\}_{j=1}^M$. For each sample x_i , a router with parameters θ produces a distribution $\pi_\theta(\cdot | x_i)$ over models and selects

$$R_{\theta,i} = R(\theta, x_i) = \arg \max_{j \in \{1, \dots, M\}} \pi_\theta(m_j | x_i). \quad (\text{A1})$$

For each sample–model pair (i, j) , let $Y_{i,j}$ denote a performance indicator (e.g. correctness) and $C_{i,j}$ denote the inference cost. The global training objective can be written as the following multi-objective problem:

$$\min_{\theta} \mathbb{E} \underbrace{[-Y_{i,R_{\theta,i}}]}_{\text{performance risk}} + \lambda \mathbb{E} \underbrace{[C_{i,R_{\theta,i}}]}_{\text{expected cost}}, \quad (\text{A2})$$

where $\lambda \geq 0$ controls the strength of the cost penalty.

To derive a cost-aware soft target, we first relax the hard decision $R_{\theta,i}$ to a distribution over models at each sample. For a fixed sample x_i , instead of choosing a single model, we consider a probability vector $q_i = (q_i(1), \dots, q_i(M)) \in \mathbb{R}^M$, $\sum_{j=1}^M q_i(j) = 1$. A natural sample-wise relaxation of (A2) is then

$$\min_{q_i \in \mathbb{R}^M} \sum_{j=1}^M q_i(j) (-Y_{i,j} + \lambda C_{i,j}), \quad (\text{A3})$$

which trades off performance and cost in expectation at x_i .

To encourage non-degenerate, smooth distributions, we

add an entropy regularizer with temperature $\tau > 0$:

$$\min_{q_i \in \mathbb{R}^M} \sum_{j=1}^M q_i(j) (-Y_{i,j} + \lambda C_{i,j}) - \tau H(q_i), \quad (\text{A4})$$

where $H(q_i) = -\sum_{j=1}^M q_i(j) \log q_i(j)$ is the Shannon entropy. We now show that, under the assumption that incorrect models are forbidden, the unique minimizer of (A4) coincides with a cost-weighted soft label supported only on correct models.

Fix a sample x_i and let

$$\mathcal{S}_i = \{j \in \{1, \dots, M\} : Y_{i,j} = 1\} \quad (\text{A5})$$

be the set of models that are correct on x_i . Assume $\mathcal{S}_i \neq \emptyset$ and that incorrect models are forbidden, *i.e.* $q_i(j) = 0$ whenever $Y_{i,j} = 0$. Consider the entropy-regularized problem

$$\min_{q_i \in \mathbb{R}^M} \sum_{j=1}^M q_i(j) (1 - Y_{i,j} + \lambda C_{i,j}) - \tau H(q_i), \quad (\text{A6})$$

with $\tau > 0$. Then the unique minimizer q_i^* satisfies

$$q_i^*(j) = \begin{cases} \frac{\exp(-\alpha C_{i,j})}{\sum_{k \in \mathcal{S}_i} \exp(-\alpha C_{i,k})}, & \text{if } j \in \mathcal{S}_i, \\ 0, & \text{otherwise,} \end{cases} \quad (\text{A7})$$

where $\alpha = \lambda/\tau > 0$. In particular, q_i^* coincides with the **cost-aware soft label** $t_i^{(\lambda)}(j)$ under $\tau = 1$ defined by

$$t_i^{(\lambda)}(j) = \begin{cases} \frac{\exp(-\lambda C_{i,j})}{\sum_{k \in \mathcal{S}_i} \exp(-\lambda C_{i,k})}, & \text{if } Y_{i,j} = 1, \\ 0, & \text{otherwise,} \end{cases} \quad (\text{A8})$$

since only correct models contribute to the denominator.

Proof. Because incorrect models are useless for training router, we may restrict q_i to be supported on \mathcal{S}_i . Define the restricted simplex

$$\Delta_i^+ = \{q_i : q_i(j) \geq 0, q_i(j) = 0 \forall j \notin \mathcal{S}_i\}. \quad (\text{A9})$$

For $j \notin \mathcal{S}_i$ we have $Y_{i,j} = 0$, and under the constraint $q_i(j) = 0$ these terms do not affect the optimization. On \mathcal{S}_i , we have $Y_{i,j} = 1$ and therefore

$$1 - Y_{i,j} = 0, \quad \forall j \in \mathcal{S}_i. \quad (\text{A10})$$

Thus, on Δ_i^+ the objective in (A6) simplifies to

$$\tilde{\mathcal{L}}_i(q_i) = \sum_{j \in \mathcal{S}_i} q_i(j) \lambda C_{i,j} - \tau H(q_i), \quad (\text{A11})$$

up to an additive constant that does not depend on q_i . Since $H(q_i)$ is strictly concave and the linear term in q_i is convex,

the objective $\tilde{\mathcal{L}}_i$ is strictly convex on Δ_i^+ , and hence has a unique minimizer.

We now compute this minimizer via Lagrange multipliers. Introduce a scalar multiplier μ for the normalization constraint $\sum_{j \in \mathcal{S}_i} q_i(j) = 1$. The Lagrangian is

$$\mathcal{J}(q_i, \mu) = \sum_{j \in \mathcal{S}_i} q_i(j) \lambda C_{i,j} - \tau H(q_i) + \mu \left(\sum_{j \in \mathcal{S}_i} q_i(j) - 1 \right). \quad (\text{A12})$$

Taking the derivative with respect to $q_i(j)$ for $j \in \mathcal{S}_i$ and setting it to zero yields

$$\frac{\partial \mathcal{J}}{\partial q_i(j)} = \lambda C_{i,j} - \tau(1 + \log q_i(j)) + \mu = 0. \quad (\text{A13})$$

Rearranging gives

$$\log q_i(j) = \frac{\mu - \lambda C_{i,j}}{\tau} - 1, \quad (\text{A14})$$

so that

$$q_i(j) = \exp\left(\frac{\mu}{\tau} - 1\right) \exp\left(-\frac{\lambda}{\tau} C_{i,j}\right) = Z_i^{-1} \exp(-\alpha C_{i,j}), \quad (\text{A15})$$

where we set $\alpha = \lambda/\tau$ and $Z_i = \exp(1 - \mu/\tau)$ is a normalization constant independent of j . Imposing the simplex constraint $\sum_{j \in \mathcal{S}_i} q_i(j) = 1$ determines Z_i as

$$Z_i = \sum_{k \in \mathcal{S}_i} \exp(-\alpha C_{i,k}). \quad (\text{A16})$$

Therefore the unique minimizer q_i^* is

$$q_i^*(j) = \begin{cases} \frac{\exp(-\alpha C_{i,j})}{\sum_{k \in \mathcal{S}_i} \exp(-\alpha C_{i,k})}, & j \in \mathcal{S}_i, \\ 0, & j \notin \mathcal{S}_i, \end{cases} \quad (\text{A17})$$

which establishes (A7). Finally, note that

$$\sum_{k \in \mathcal{M}} e^{-\alpha C_{i,k}} = \sum_{k \in \mathcal{S}_i} e^{-\alpha C_{i,k}} \quad (\text{A18})$$

since all terms with $k \notin \mathcal{S}_i$ vanish after multiplying by the indicator $\mathbf{1}_{Y_{i,k}=1}$ in the definition of $t_i^{(\lambda)}(j)$. Hence $q_i^*(j)$ coincides with $t_i^{(\lambda)}(j)$ under $\tau = 1$, completing the proof. \square

D. Pareto Frontier Fitting

To rigorously evaluate the trade-off between inference cost and generation quality, we analyze the Pareto Frontier of the routing system. While RouterBench [8] proposes a geometric approach based on the Non-Decreasing Convex Hull (NDCH), we implement a parametric exponential saturation

model to characterize the diminishing returns of computational investment and estimating the theoretical performance ceiling.

We approximate the Pareto frontier using a smooth exponential saturation function. Let x denote the average cost and y denote the average accuracy. We fit the empirical data to the following non-linear equation:

$$y(x) = a \cdot (1 - e^{-b \cdot x}) + c \quad (\text{A19})$$

where c represents the floor performance approximated by the minimum performance in the Pareto set. $a + c$ represents the asymptotic maximum performance that the routing strategy could theoretically achieve given an infinite budget. b is the shape parameter and a larger b indicates high marginal utility in the low-cost regime, characterizing a highly efficient router.

We perform curve fitting using the Trust Region Reflective algorithm to minimize the least squares error. To ensure robust convergence, we initialize the parameters based on the empirical Pareto points, and the goodness of fit is validated using the coefficient of determination.

E. Detailed Information about the Datasets

E.1. General

- **MMBench** [14]

MMBench provides a robust evaluation of 20 fine-grained skills using 3,217 meticulously balanced questions. It introduces a novel CircularEval strategy and uses GPT-4 for answer matching to ensure a comprehensive and robust assessment of multi-modal abilities.

- **MMStar** [15]

MMStar is an elite "vision-indispensable" multi-modal benchmark comprising 1,500 meticulously human-selected samples, covering 6 core capabilities and 18 detailed axes. The dataset is designed to rigorously evaluate Large VLMs by eliminating samples that can be solved without visual input, thereby addressing data leakage and ensuring true multi-modal competency.

- **MMMU** [16]

MMMU evaluates multimodal models on massive multi-discipline tasks demanding college-level knowledge and deliberate reasoning. It comprises 11.5K questions across six core disciplines and 30 heterogeneous image types, challenging models with expert-level content akin to professional exams.

- **RealWorldQA** [17]

RealWorldQA is a benchmark designed for evaluating basic real-world spatial understanding capabilities of multimodal models. The dataset comprises 765 images.

- **InfoVQA** [18]

InfoVQA benchmarks the understanding of complex infographics, requiring joint reasoning over layout, textual

content, and graphical elements. With 30,035 questions across 5,485 images, it specifically challenges models to perform elementary reasoning on diverse data visualizations, bridging the gap between computer vision and document understanding.

- **HallusionBench** [39]

HallusionBench stands out as a diagnostic suite tailored to dissect "Language Hallucination \times Visual Illusion" failure modes. Comprising 1,129 handcrafted VQA pairs, it utilizes a unique structure of original versus expert-modified images to test visual dependency rigorously. This approach moves beyond simple accuracy to quantitatively analyze specific failure dimensions.

E.2. STEM

- **MathVista** [19]

MathVista combines diverse mathematical and visual challenges to evaluate fine-grained visual understanding and compositional reasoning. Integrating 28 existing and three new datasets, it covers 6,141 examples across varied visual contexts and seven distinct reasoning types.

- **MathVision** [20]

MathVision offers 3,040 high-quality visual math problems meticulously selected from 19 math competitions across 12 grades. Strictly cross-validated by experts, it balances open-ended and multiple-choice formats, covering 16 mathematical disciplines to measure reasoning depth.

- **MathVerse** [21]

MathVerse assesses genuine visual diagram understanding by transforming problems into six versions with varying multi-modal information. It features 2,612 problems across geometry and functions, employing a novel Chain-of-Thought (CoT) evaluation strategy for fine-grained reasoning assessment.

- **AI2D** [22]

AI2D addresses diagram interpretation using over 5,000 grade-school science diagrams. It uniquely employs Diagram Parse Graphs (DPG) to model syntactic structure and semantic relationships. With 150,000 rich annotations and 15,000 multiple-choice questions, it challenges models to decode visual symbolism—such as arrows indicating process flow versus consumption—beyond simple object recognition.

E.3. Chart OCR

- **TextVQA** [25]

TextVQA challenges models to read and reason about text embedded within images to answer questions. Comprising 45,336 human-generated questions across 28,408 text-rich images (e.g., billboards, signs) from the Open Images dataset, the benchmark requires integrating optical character recognition (OCR) with semantic reasoning to address complex queries involving scene text.

- **ChartQA** [23]
ChartQA addresses the limitations of synthetic datasets by evaluating visual and logical reasoning on 20,882 real-world charts collected from diverse online sources. It combines 9,608 human-written questions with 23,111 questions generated from summaries, overcoming issues of fixed vocabularies and template-based queries to support complex reasoning tasks involving aggregation and comparison.
- **DocVQA** [24]
DocVQA drives a “purpose-driven” approach to document analysis, featuring 50,000 questions across 12,767 diverse industry documents (e.g., forms, letters) from the UCSF Library. It challenges models to move beyond simple text extraction, requiring the interpretation of complex layouts, handwriting, and non-textual elements to retrieve information effectively.
- **OCRBench** [26]
OCRBench is a comprehensive benchmark tailored to evaluate the OCR capabilities of Large Multimodal Models. It comprises 1,000 manually verified question-answer pairs spanning five diverse components: text recognition, scene-text VQA, document VQA, key information extraction, and handwritten mathematical expressions. This design rigorously tests models on identifying and reasoning with text across varied visual contexts, from artistic fonts to complex documents.

F. Detailed Information about the Models

F.1. Open-source models

- **DeepSeek-VL2** [41]
DeepSeek-VL2 (Basic) is a Mixture-of-Experts vision–language model featuring a total of 27B parameters, with roughly 4.5B parameters activated during inference. It offers a strong and competitive open-source baseline, serving as a higher-capacity counterpart to its Tiny variant.
Official release: <https://github.com/deepseek-ai/DeepSeek-VL2>
- **DeepSeek-VL2-Tiny** [41]
A cost-efficient MoE variant with 27B total parameters but only 1B activated per token. It maintains reasonable multimodal performance while significantly reducing computational cost.
Official release: <https://github.com/deepseek-ai/DeepSeek-VL2>
- **Gemma3-27B** [48]
A 27B dense VLM based on the Gemma3 architecture, offering strong general multimodal performance and serving as a competitive upper-tier open-source model.
Official release: <https://github.com/google-deepmind/gemma>
- **InternVL2.5-78B** [49]

A 78B high-capacity VLM with advanced vision processing and strong reasoning ability. It is the largest model in our open-source pool and enriches the high-end of the Pareto frontier.

Official release: <https://github.com/OpenGVLab/InternVL>

- **Janus-Pro-1B** [40]

A lightweight 1B VLM designed for cost-sensitive scenarios. Its compact transformer and ViT structure make it suitable as an extremely efficient routing candidate.

Official release: <https://github.com/deepseek-ai/Janus>

- **Janus-Pro-7B** [40]

A 7B dense VLM equipped with a larger language backbone and a more capable vision encoder than the 1B variant, representing a standard mid-sized open-source model.

Official release: <https://github.com/deepseek-ai/Janus>

- **Kimi-VL-A3B-Thinking-2506** [43]

A reasoning-optimized MoE VLM with 2.8B activated parameters. Although efficient, it often produces longer output sequences due to its “thinking-mode” tuning.

Official release: <https://github.com/MoonshotAI/Kimi-VL>

- **LLaVA-Next-Vicuna-7B** [36]

A popular LLaVA-style baseline built on Vicuna-7B with a CLIP-like vision encoder. It performs well on standard VQA and everyday multimodal tasks.

Official release: <https://github.com/LLaVA-VL/LLaVA-NeXT>

- **MiMo-VL-7B-RL** [45]

A 7B VLM improved with reinforcement learning to encourage more deliberate reasoning. It provides an alternative training paradigm compared with purely supervised LLaVA models.

Official release: <https://github.com/InternLM/MiMo>

- **Phi-3.5-Vision** [44]

A vision-augmented version of the Phi-3.5 language model, using a SigLIP-style vision encoder. It demonstrates strong efficiency and STEM-oriented reasoning performance.

Official release: <https://github.com/microsoft/Phi-3>

- **Pixtral-12B** [47]

A 12B dense VLM offering competitive performance in document understanding and visual reasoning. It provides a middle-high capacity option between 7B and 27B models.

Official release: <https://huggingface.co/mistralai/Pixtral>

- **Qianfan-VL-8B** [46]

An 8B instruction-tuned VLM from Baidu Qianfan, filling the performance gap between 7B and 12B models and enhancing diversity in the mid-range model pool.

Official release: <https://qianfan.cloud.baidu.com>

- **Qwen2.5-VL-32B-Instruct** [27]

A 32B VLM equipped with resolution-adaptive visual tokenization, making input cost sensitive to image size. It provides high accuracy and strong general reasoning.

Official release: <https://github.com/QwenLM/Qwen2.5-VL>

- **Qwen2.5-VL-72B-Instruct** [27]

A 72B flagship model offering state-of-the-art open-source multimodal reasoning. It is one of the most powerful open-source models in our evaluation.

Official release: <https://github.com/QwenLM/Qwen2.5-VL>

- **SmolVLM2** [42]

A 2.2B compact VLM combining a CLIP-based vision encoder with a lightweight language model. It strikes a balance between cost and performance and strengthens the low-to-mid capacity tier.

Official release: <https://huggingface.co/SmolVLM>

F.2. API models

- **Gemini-Flash-2.5** [50]

A closed-source multimodal model accessed through API, optimized for high throughput and low latency. Token usage and cost follow the official API billing.

Documentation: <https://ai.google.dev/gemini-api>

- **GPT-4o** [51]

A frontier multimodal model from OpenAI providing top-tier performance with relatively low input cost but high output-token cost. Token usage is taken directly from API response metadata.

Documentation: <https://platform.openai.com/docs>

G. Detailed Information about the Routing Methods

G.1. Router Strategy

- **K-Nearest Neighbors (KNN)** [52]

We implement a similarity-based router using the KNN algorithm, extending the text-based routing approach to the multimodal domain. The core basis is that queries sharing similar visual and textual semantic features should be best served by the same underlying VLM.

- **Pairwise Preference Aggregated KNN (PRkNN)** [53]

Unlike the standard KNN router which relies on a single “hard” label per training sample, discarding information

about second-best options or close calls, PRkNN utilizes the full correctness matrix and cost matrix of the retrieved neighbors to perform a fine-grained pairwise comparison.

- **One-vs-Rest (OVR)** [54]

We implement a decompositional routing strategy based on the One-vs-Rest (OVR) framework. OVR treats the routing problem as a set of K independent binary classification tasks, where K is the number of candidate models in the pool. It assumes that the “best” model is the one with the highest independent probability of correctness, effectively maximizing the expected accuracy.

- **K-means** [52]

We implement a similarity-based routing approach using K class means, where K is the number of models and a nearest centroid classifier. Instead of storing all training samples, this method aggregates the multimodal features of queries and images best suited for a specific model into a single representative vector. This method significantly reduces inference latency, as it requires only K dot products, rather than searching the entire training database.

- **Linear** [52]

We implement a parametric routing baseline, Linear, which treats the model selection task as a standard multi-class classification problem. Linear learns a global linear decision boundary in the multimodal feature space. Given the fused feature vector $\mathbf{x} \in \mathbb{R}^d$, the router computes a probability distribution \mathbf{p} over the K candidate models via a linear transformation followed by the Softmax function.

- **Multi-Layer Perceptron (MLP)** [52]

We implement a non-linear parametric router using a Multi-Layer Perceptron (MLP), which serves as a more expressive alternative to the linear baseline [52]. This method learns a non-linear mapping from the multimodal feature space to the model selection probability distribution, capturing complex interactions between visual and textual semantics.

- **Cosine Classifier (CosineCls)** [4]

We implement a metric-based routing approach that learns a shared embedding space for both queries and candidate models, leveraging the architecture and Sample-LLM contrastive learning objective proposed in the Cosine Classifier framework [4] to VLM Router. Cosine method fine-tunes a Transformer encoder, to align user queries directly with learnable model prototypes based on semantic suitability.

- **Dual-Contrastive Router(RouterDC)** [4]

We implement the RouterDC framework to VLM Router, which extends the previously described Cosine Classifier by incorporating a dual-contrastive learning objective. While the Cosine Classifier focuses solely on aligning queries with model prototypes (Sample-LLM alignment), RouterDC introduces an auxiliary Sample-Sample objective to regularize the embedding space by preserving the

semantic manifold structure of the queries.

- **Zooter [33]**

We implement Zooter, an end-to-end routing framework that fine-tunes a pre-trained Transformer encoder to predict optimal model selection directly from raw text and vision queries, eliminating the need for fixed, pre-extracted embeddings. The router employs a standard Transformer encoder architecture followed by a classification head. Zooter supports both hard and soft label training regimes to balance performance and cost.

G.2. Fusion Method

Let the visual embedding be denoted as $\mathbf{v} \in \mathbb{R}^{d_v}$ and the textual embedding as $\mathbf{q} \in \mathbb{R}^{d_q}$. We implement the following fusion strategies to construct a unified representation \mathbf{f} for the routing policy.

- **Concatenation**

This method preserves the full information from both modalities by joining the vectors along the channel dimension. The fused representation is defined as:

$$\mathbf{f}_{\text{concat}} = [\mathbf{v}; \mathbf{q}] \in \mathbb{R}^{d_v + d_q} \quad (\text{A20})$$

where $[\cdot; \cdot]$ represents the concatenation operation.

- **Normalized Concatenation**

To mitigate scale discrepancies between the visual and textual encoders, we apply L_2 normalization to each embedding prior to concatenation:

$$\mathbf{f}_{\text{norm-concat}} = \left[\frac{\mathbf{v}}{\|\mathbf{v}\|_2}; \frac{\mathbf{q}}{\|\mathbf{q}\|_2} \right] \quad (\text{A21})$$

- **Weighted Average**

To allow the model to adaptively prioritize one modality (e.g., text-dominant vs. image-dominant queries), we introduce a learnable scalar coefficient $\alpha \in [0, 1]$:

$$\mathbf{f}_{\text{w-avg}} = \alpha \mathbf{v} + (1 - \alpha) \mathbf{q} \quad (\text{A22})$$

- **Gated Multimodal Unit (GMU) [64]**

This approach uses a learnable gating mechanism to control the information flow from each modality per sample. We compute a gate vector \mathbf{z} via a sigmoid activation σ :

$$\mathbf{z} = \sigma(W_z^v \mathbf{v} + W_z^q \mathbf{q} + \mathbf{b}_z) \quad (\text{A23})$$

The final fused representation combines the transformed features using \mathbf{z} as a soft switch:

$$\mathbf{f}_{\text{GMU}} = \mathbf{z} \odot \tanh(W_v \mathbf{v}) + (1 - \mathbf{z}) \odot \tanh(W_q \mathbf{q}) \quad (\text{A24})$$

where \odot denotes the element-wise product.

- **Multimodal Low-rank Bilinear (MLB) Fusion [65]**

To capture multiplicative interactions between modalities efficiently, MLB projects the inputs into a common space

and fuses them via element-wise multiplication (Hadamard product):

$$\mathbf{h} = \sigma(W_v^T \mathbf{v}) \odot \sigma(W_q^T \mathbf{q}) \quad (\text{A25})$$

where σ is typically the hyperbolic tangent (\tanh) function. The final routing prediction is obtained by passing this fused representation through a linear classifier:

$$\hat{y} = \text{softmax}(W_{\text{MLP}} \mathbf{h} + \mathbf{b}_{\text{MLP}}) \quad (\text{A26})$$

G.3. Router Backbone

We use pretrained transformer models in multiple methods like Cosine Classifier [4], RouterDC [4], Zooter [33], etc. We select BERT [66], MobileNetV4 [67], VisualBERT [55], UNITER [56], LXMERT [57] and VILBERT [58] as different backbones for experiment and choose the best one to combine with these methods, which turns out to be LXMERT.

- **BERT [66]**

We use BERT as the text-only backbone for our end-to-end router. BERT’s key innovation is its ability to learn representations by conditioning on both left and right context through two pre-training objectives: Masked Language Modeling (MLM), which randomly masks 15% of input tokens and predicts the original vocabulary based on context, and Next Sentence Prediction (NSP), a binary classification task to predict whether sentence B follows sentence A . The special $[\text{CLS}]$ token at the beginning of each sequence provides an aggregate representation, $\mathbf{h}_{[\text{CLS}]}$, which is used for classification to predict the optimal model index.

- **MobileNetV4 [67]**

We use MobileNetV4 as the image-only backbone for our end-to-end router. MobileNetV4’s key innovation is the Universal Inverted Bottleneck (UIB) block, which combines the classical Inverted Bottleneck (IB) and ConvNext-style block into a flexible component. The UIB adapts during architecture search, enabling it to function as an IB, ConvNext block, or Feed-Forward Network (FFN) to optimize performance across diverse hardware. To capture long-range dependencies without the overhead of traditional Self-Attention, MobileNetV4 introduces Mobile MQA (Multi-Query Attention), which shares keys and values across attention heads to reduce memory bandwidth demands while preserving global context modeling. This hybrid architecture strikes an excellent balance between latency and accuracy, making MobileNetV4 ideal for real-time routing with minimal inference overhead.

- **VisualBERT [55]**

We use VisualBERT as a text-image backbone, representing “single-stream” multimodal architectures. VisualBERT’s key feature is its unified modeling approach, where visual tokens (derived from images) are directly concatenated with text embeddings and processed through a single stack of Transformer layers. This design enables

early fusion, allowing deep, self-attention-based interaction between text tokens and image regions at every layer. Compared to late-fusion models, VisualBERT captures fine-grained grounding more effectively, while leveraging pre-trained BERT weights to accelerate convergence.

- **UNITER** [56]

We adopt UNITER, a unified Transformer model for joint image-text representation learning. Through pre-training on tasks like Masked Language Modeling, Image-Text Matching, and Word-Region Alignment (via Optimal Transport), it achieves robust cross-modal alignment. UNITER’s universal representations enable strong zero-shot or fine-tuned performance on diverse downstream tasks using a single set of weights.

- **LXMERT** [57]

We employ LXMERT as a representative dual-stream architecture for multimodal fusion. It processes vision and language inputs separately before fusing them through a cross-modality encoder. This design enables strong unimodal representation learning and excels in complex reasoning tasks like VQA.

- **VILBERT** [58]

We utilize ViLBERT, a dual-stream architecture that extends BERT to multimodal data. It processes vision and language in separate Transformer streams, interacting through co-attentional layers. These layers use cross-modal attention (e.g., vision queries attend to language keys/values) to enable context-aware fusion while preserving modality-specific representations.

H. Implementation Details

All trainable routers in our benchmark share the same data pipeline and optimization protocol, independent of the specific architecture (feature-level routers or end-to-end routers). We start from the VL-RouterBench logs, which provide for each sample $x_i = (I_i, T_i)$ a binary or real-valued quality vector $Y_i \in \mathbb{R}^M$ over the M candidate models and a corresponding cost vector $C_i \in \mathbb{R}^M$. The full quality and cost matrices are denoted by $Y \in \mathbb{R}^{N \times M}$ and $C \in \mathbb{R}^{N \times M}$, where N is the number of samples. We use the pre-defined `train/dev/test` splits, with the ratio $|\mathcal{D}_{\text{tr}}| : |\mathcal{D}_{\text{dev}}| : |\mathcal{D}_{\text{te}}| = 7 : 1 : 2$.

To supervise the router, we derive either hard or soft training targets over the M experts from (Y_i, C_i) via the multi-objective formulation in Sec. 3.3. Concretely, we compute a target distribution that concentrates probability mass on models with high quality and low cost, controlled by a trade-off parameter λ . We use a set of $\lambda = [0.0, 10.0, 100.0, 1000.0, 10000.0, +\infty]$ in the experiments to control the trade-off between accuracy and cost. For feature-level routers we first compute a fixed text embedding for T_i and then train a shallow classifier on top. For end-to-end routers we attach a task-specific classification

head to the final [CLS] or pooled multimodal representation of the visual-language backbone. Unless otherwise specified, we train all routers with AdamW, a learning rate of 2×10^{-5} , batch size 16, and weight decay 0.01, using a cosine decay schedule thereafter. We train for at most 5 epochs. For Linear, MLP, CosineCls, RouterDC, ZOOTER, and VLC, results in main experiments are presented as mean and standard deviation across 5 independent trials.

I. Additional Experiments

I.1. Results on Oracle and Models

We provide the detailed results of all candidate models and the Oracle router on VL-RouterBench in Fig. A1. The Oracle represents an ideal routing policy and achieves the highest average accuracy at very low average cost, which highlights the substantial potential of routing systems for improving the cost effectiveness of VLM deployments. It is also noteworthy that the two API models, despite their significantly higher prices, do not obtain better average accuracy than several cheaper open source candidates. This pattern poses a challenge for practical router design, since an effective routing strategy must explicitly avoid high cost options whose accuracy does not justify their price and instead maintain a favorable balance between accuracy and cost.

I.2. Detailed Results on Each Dataset

We further report per-dataset detailed results under different values of λ , as shown in Tab. A1–Tab. A6. These tables characterize the accuracy-cost trade-offs achieved by different routing methods across a wide range of λ , providing a fine-grained view of how each method adapts under varying cost preferences.

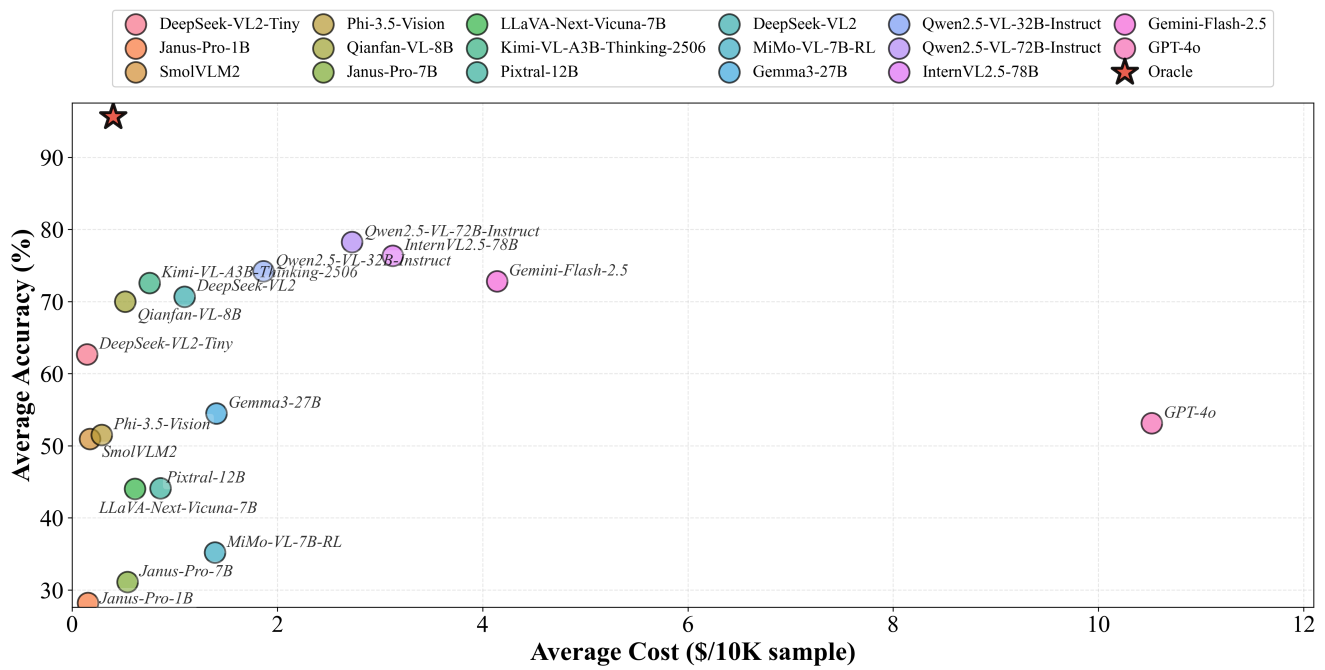


Figure A1. Accuracy-Cost Curve of Oracle and Models. The closer to the upper left corner, the better the accuracy-cost trade-off.

Table A1. Performance comparison of router methods on VL-RouterBench across datasets for $\lambda = 0.0$. **Avg. Acc.** is average accuracy (%), **Avg. Cost** is average cost (\$/10K samples). The best and second-best results among learned routers are highlighted in **bold** and underlined, respectively (excluding Oracle and baseline methods).

Group	Dataset	Metric	Baselines			Hard Label				Soft Label ($\lambda = 0.0$)					
			Oracle	Strongest	Cheapest	KNN	PRkNN	OVR	K-means	Linear	MLP	CosineCls	RouterDC	VLC	ZOOTER
General	HallusionBench	Avg. Acc. \uparrow	99.46	71.89	57.84	40.54	43.24	66.49	70.27	68.65	68.65	<u>79.46</u>	80.00	67.03	71.89
		Avg. Cost \downarrow	0.23	2.97	0.14	0.18	<u>0.21</u>	1.67	2.89	2.17	3.02	4.18	2.82	3.03	2.16
	InfoVQA	Avg. Acc. \uparrow	96.49	83.28	53.68	58.36	61.87	<u>81.10</u>	80.60	77.93	81.10	80.60	81.10	82.61	80.77
		Avg. Cost \downarrow	0.37	2.19	0.14	0.24	<u>0.29</u>	1.49	2.09	1.66	1.73	0.99	1.12	1.20	1.61
	MMBench	Avg. Acc. \uparrow	98.16	89.86	69.59	69.59	81.11	85.25	70.97	82.95	87.56	90.32	<u>90.32</u>	87.10	84.79
		Avg. Cost \downarrow	0.24	2.22	0.13	0.19	<u>0.27</u>	2.26	1.17	1.55	1.90	5.33	2.52	1.84	1.57
STEM	MMMU	Avg. Acc. \uparrow	98.46	74.36	45.64	42.05	53.33	60.00	65.64	67.69	<u>76.92</u>	77.44	76.41	75.38	72.31
		Avg. Cost \downarrow	0.64	3.24	0.17	0.41	<u>0.43</u>	6.95	10.59	11.33	13.22	17.54	7.06	12.91	10.65
	MMStar	Avg. Acc. \uparrow	96.68	72.76	49.17	54.48	59.80	68.44	66.11	63.46	70.76	75.08	72.76	69.44	<u>74.75</u>
		Avg. Cost \downarrow	0.36	2.29	0.14	0.25	<u>0.29</u>	2.85	1.68	1.76	2.78	7.98	8.26	2.58	2.78
	RealWorldQA	Avg. Acc. \uparrow	99.32	77.40	67.12	55.48	63.70	67.81	60.27	69.86	69.86	<u>78.08</u>	77.40	74.66	80.14
		Avg. Cost \downarrow	0.22	2.20	0.13	0.14	<u>0.18</u>	1.46	1.17	1.15	1.84	3.55	3.77	2.27	1.78
Chart & Doc	AI2D	Avg. Acc. \uparrow	99.69	88.21	72.33	67.45	73.58	80.66	76.42	76.10	83.80	87.11	<u>86.95</u>	82.70	84.43
		Avg. Cost \downarrow	0.24	2.19	0.13	0.16	<u>0.19</u>	2.05	2.56	1.20	2.94	7.17	2.10	2.02	2.40
	MathVerse	Avg. Acc. \uparrow	90.36	49.74	23.05	59.77	67.97	68.75	66.93	69.53	71.09	62.37	66.15	<u>69.92</u>	52.99
		Avg. Cost \downarrow	1.06	4.67	0.18	1.64	<u>1.70</u>	4.01	3.19	3.99	4.04	7.85	2.59	3.87	2.55
	MathVision	Avg. Acc. \uparrow	89.55	38.81	13.43	28.36	23.88	35.82	46.27	49.25	50.75	61.19	<u>61.19</u>	50.75	61.19
		Avg. Cost \downarrow	1.77	8.16	0.17	<u>1.23</u>	0.72	13.10	5.64	9.92	15.50	26.73	2.73	19.30	24.39
Average	MathVista	Avg. Acc. \uparrow	95.85	75.13	51.30	53.89	70.98	77.20	73.58	72.54	<u>79.27</u>	76.68	77.20	76.17	79.79
		Avg. Cost \downarrow	0.36	5.00	0.16	0.50	<u>0.54</u>	3.46	2.81	3.79	4.82	9.52	6.67	3.54	4.45
	ChartQA	Avg. Acc. \uparrow	97.80	86.20	81.00	81.40	80.80	81.00	40.60	70.20	83.80	70.60	76.40	<u>83.20</u>	82.60
		Avg. Cost \downarrow	0.21	2.19	0.14	0.14	<u>0.17</u>	1.09	0.69	0.38	0.98	1.74	0.86	1.30	1.34
	DocVQA	Avg. Acc. \uparrow	98.56	91.48	78.95	78.66	80.48	85.55	82.30	80.19	<u>88.13</u>	87.85	88.04	87.37	89.57
		Avg. Cost \downarrow	0.18	2.18	0.14	0.15	<u>0.18</u>	1.22	1.25	0.58	1.34	0.98	0.21	1.34	1.41
All Datasets	OCRBench	Avg. Acc. \uparrow	99.06	89.20	80.28	77.00	81.22	85.92	79.34	81.22	86.85	<u>93.90</u>	94.37	89.67	87.32
		Avg. Cost \downarrow	0.23	2.41	0.14	0.16	<u>0.19</u>	1.44	0.96	0.71	1.61	1.60	0.68	1.77	1.70
	TextVQA	Avg. Acc. \uparrow	89.46	73.85	72.13	70.98	<u>72.13</u>	67.05	66.09	68.29	71.26	67.62	68.49	73.56	69.73
All Datasets		Avg. Cost \downarrow	0.18	2.15	0.13	0.14	<u>0.16</u>	1.12	1.81	0.33	1.86	1.31	0.84	1.41	0.78
	All Datasets	Avg. Acc. \uparrow	95.60	78.01	62.43	66.26	70.68	75.49	70.01	73.08	<u>78.62</u>	77.19	78.24	78.65	76.70
		Avg. Cost \downarrow	0.37	2.72	0.14	0.38	<u>0.41</u>	2.18	2.21	1.82	2.75	3.37	1.14	2.53	2.32
		Rank Score \uparrow	93.68	68.88	64.63	67.13	<u>71.09</u>	68.92	64.62	68.23	69.19	65.90	74.81	70.04	69.36

Table A2. Performance comparison of router methods on VL-RouterBench across datasets for $\lambda = 10.0$. **Avg. Acc.** is average accuracy (%), **Avg. Cost** is average cost (\$/10K samples). The best and second-best results among learned routers are highlighted in **bold** and underlined, respectively (excluding Oracle and baseline methods).

Group	Dataset	Metric	Baselines			Hard Label				Soft Label ($\lambda = 10.0$)					
			Oracle	Strongest	Cheapest	KNN	PRkNN	OVR	K-means	Linear	MLP	CosineCls	RouterDC	VLC	ZOOTER
General	HallusionBench	Avg. Acc. \uparrow	99.46	71.89	57.84	40.54	43.24	66.49	70.27	73.51	65.95	61.08	58.38	<u>70.81</u>	65.41
		Avg. Cost \downarrow	0.23	2.97	0.14	<u>0.18</u>	0.21	1.67	2.89	3.13	0.98	0.17	0.19	0.90	1.49
	InfoVQA	Avg. Acc. \uparrow	96.49	83.28	53.68	58.36	61.87	<u>81.10</u>	80.60	72.41	78.60	57.19	65.05	83.11	80.43
		Avg. Cost \downarrow	0.37	2.19	0.14	0.24	0.29	1.49	2.09	0.87	1.31	<u>0.24</u>	0.43	2.00	1.72
	MMBench	Avg. Acc. \uparrow	98.16	89.86	69.59	69.59	81.11	85.25	70.97	82.95	89.86	77.42	79.72	88.02	<u>89.86</u>
		Avg. Cost \downarrow	0.24	2.22	0.13	0.19	0.27	2.26	1.17	2.44	1.08	<u>0.24</u>	0.28	0.93	1.62
STEM	MMMU	Avg. Acc. \uparrow	98.46	74.36	45.64	42.05	53.33	60.00	<u>65.64</u>	70.77	58.46	48.21	51.79	62.05	60.00
		Avg. Cost \downarrow	0.64	3.24	0.17	0.41	0.43	6.95	10.59	11.64	1.59	<u>0.33</u>	0.31	1.08	1.16
	MMStar	Avg. Acc. \uparrow	96.68	72.76	49.17	54.48	59.80	68.44	66.11	67.44	69.10	56.81	59.14	<u>69.77</u>	70.43
		Avg. Cost \downarrow	0.36	2.29	0.14	0.25	0.29	2.85	1.68	2.33	1.05	0.24	<u>0.24</u>	0.83	1.33
	RealWorldQA	Avg. Acc. \uparrow	99.32	77.40	67.12	55.48	63.70	67.81	60.27	67.12	69.86	63.70	61.64	<u>71.92</u>	79.45
		Avg. Cost \downarrow	0.22	2.20	0.13	0.14	0.18	1.46	1.17	1.91	0.70	<u>0.16</u>	0.31	1.27	1.29
Chart & Doc	AI2D	Avg. Acc. \uparrow	99.69	88.21	72.33	67.45	73.58	80.66	76.42	79.56	83.02	73.58	72.80	86.16	<u>84.28</u>
		Avg. Cost \downarrow	0.24	2.19	0.13	0.16	0.19	2.05	2.56	2.20	1.10	<u>0.17</u>	0.21	1.50	1.37
	MathVerse	Avg. Acc. \uparrow	90.36	49.74	23.05	59.77	<u>67.97</u>	68.75	66.93	67.71	69.92	64.71	57.68	62.11	64.32
		Avg. Cost \downarrow	1.06	4.67	0.18	<u>1.64</u>	1.70	4.01	3.19	3.33	3.28	3.92	2.39	1.52	2.18
	MathVision	Avg. Acc. \uparrow	89.55	38.81	13.43	28.36	23.88	35.82	46.27	46.27	49.25	49.25	37.31	52.24	<u>52.24</u>
		Avg. Cost \downarrow	1.77	8.16	0.17	1.23	0.72	13.10	5.64	7.07	2.55	9.16	<u>1.17</u>	1.78	1.78
Average	MathVista	Avg. Acc. \uparrow	95.85	75.13	51.30	53.89	70.98	77.20	73.58	76.17	81.87	62.69	62.18	<u>77.72</u>	77.72
		Avg. Cost \downarrow	0.36	5.00	0.16	<u>0.50</u>	0.54	3.46	2.81	3.72	1.90	0.77	0.44	1.14	1.17
	ChartQA	Avg. Acc. \uparrow	97.80	86.20	81.00	81.40	80.80	81.00	40.60	79.40	<u>84.00</u>	82.40	83.40	87.00	81.20
		Avg. Cost \downarrow	0.21	2.19	0.14	0.14	<u>0.17</u>	1.09	0.69	1.36	0.58	0.17	0.22	0.85	1.58
	DocVQA	Avg. Acc. \uparrow	98.56	91.48	78.95	78.66	80.48	85.55	82.30	82.78	85.07	79.14	81.24	90.14	<u>88.52</u>
		Avg. Cost \downarrow	0.18	2.18	0.14	0.15	0.18	1.22	1.25	0.62	0.65	<u>0.15</u>	0.21	1.59	1.20
All Datasets	OCRBench	Avg. Acc. \uparrow	99.06	89.20	80.28	77.00	81.22	85.92	79.34	80.28	88.26	81.22	85.45	<u>88.26</u>	85.45
		Avg. Cost \downarrow	0.23	2.41	0.14	0.16	0.19	1.44	0.96	1.18	1.06	<u>0.16</u>	0.21	<u>0.57</u>	0.97
	TextVQA	Avg. Acc. \uparrow	89.46	73.85	72.13	70.98	72.13	67.05	66.09	66.38	72.70	<u>72.41</u>	70.59	70.88	71.74
All Datasets		Avg. Cost \downarrow	0.18	2.15	0.13	0.14	0.16	1.12	1.81	1.05	0.57	<u>0.14</u>	0.17	0.62	0.31
	All Datasets	Avg. Acc. \uparrow	95.60	78.01	62.43	66.26	70.68	75.49	70.01	73.97	<u>77.32</u>	69.88	70.99	78.09	77.26
		Avg. Cost \downarrow	0.37	2.72	0.14	0.38	<u>0.41</u>	2.18	2.21	2.08	1.22	0.77	0.53	1.23	1.30
		Rank Score \uparrow	93.68	68.88	64.63	67.13	71.09	68.92	64.62	68.10	<u>73.73</u>	68.98	70.89	74.33	73.40

Table A3. Performance comparison of router methods on VL-RouterBench across datasets for $\lambda = 100.0$. **Avg. Acc.** is average accuracy (%), **Avg. Cost** is average cost (\$/10K samples). The best and second-best results among learned routers are highlighted in **bold** and underlined, respectively (excluding Oracle and baseline methods).

Group	Dataset	Metric	Baselines			Hard Label				Soft Label ($\lambda = 100.0$)					
			Oracle	Strongest	Cheapest	KNN	PRkNN	OVR	K-means	Linear	MLP	CosineCls	RouterDC	VLC	ZOOTER
General	HallusionBench	Avg. Acc. \uparrow	99.46	71.89	57.84	40.54	43.24	66.49	70.27	67.03	58.92	56.22	59.46	59.46	58.38
		Avg. Cost \downarrow	0.23	2.97	0.14	0.18	0.21	1.67	2.89	1.56	0.33	0.20	0.21	0.23	<u>0.19</u>
	InfoVQA	Avg. Acc. \uparrow	96.49	83.28	53.68	58.36	61.87	81.10	<u>80.60</u>	79.77	74.41	65.05	68.06	67.56	56.69
		Avg. Cost \downarrow	0.37	2.19	0.14	<u>0.24</u>	0.29	1.49	2.09	1.71	0.56	0.36	0.44	0.60	0.21
	MMBench	Avg. Acc. \uparrow	98.16	89.86	69.59	69.59	81.11	85.25	70.97	<u>83.41</u>	77.42	80.18	81.57	82.49	68.66
		Avg. Cost \downarrow	0.24	2.22	0.13	0.19	0.27	2.26	1.17	1.32	0.30	0.23	0.44	0.34	<u>0.20</u>
STEM	MMMU	Avg. Acc. \uparrow	98.46	74.36	45.64	42.05	53.33	60.00	<u>65.64</u>	68.72	55.90	51.28	53.85	53.33	54.87
		Avg. Cost \downarrow	0.64	3.24	0.17	0.41	0.43	6.95	10.59	10.21	0.52	<u>0.41</u>	0.45	0.50	0.49
	MMStar	Avg. Acc. \uparrow	96.68	72.76	49.17	54.48	59.80	68.44	<u>66.11</u>	62.13	64.45	60.47	58.80	60.47	61.13
		Avg. Cost \downarrow	0.36	2.29	0.14	0.25	<u>0.29</u>	2.85	1.68	2.66	0.36	0.30	0.30	0.32	0.30
	RealWorldQA	Avg. Acc. \uparrow	99.32	77.40	67.12	55.48	63.70	<u>67.81</u>	60.27	65.07	67.12	65.07	65.75	70.55	66.44
		Avg. Cost \downarrow	0.22	2.20	0.13	0.14	0.18	1.46	1.17	0.80	0.17	0.23	0.21	0.27	<u>0.15</u>
Chart & Doc	AI2D	Avg. Acc. \uparrow	99.69	88.21	72.33	67.45	73.58	<u>80.66</u>	76.42	78.14	80.82	74.53	72.01	74.53	72.96
		Avg. Cost \downarrow	0.24	2.19	0.13	0.16	<u>0.19</u>	2.05	2.56	0.91	0.36	0.25	0.21	0.22	0.23
	MathVerse	Avg. Acc. \uparrow	90.36	49.74	23.05	59.77	<u>67.97</u>	68.75	66.93	67.32	61.98	64.84	64.06	60.29	63.02
		Avg. Cost \downarrow	1.06	4.67	0.18	1.64	1.70	4.01	3.19	3.55	<u>1.60</u>	3.86	3.69	1.37	2.31
	MathVision	Avg. Acc. \uparrow	89.55	38.81	13.43	28.36	23.88	35.82	46.27	41.79	49.25	52.24	50.75	50.75	<u>52.24</u>
		Avg. Cost \downarrow	1.77	8.16	0.17	<u>1.23</u>	0.72	13.10	5.64	10.53	1.80	3.29	2.49	1.76	1.78
Average	MathVista	Avg. Acc. \uparrow	95.85	75.13	51.30	53.89	70.98	<u>77.20</u>	73.58	71.50	75.65	65.29	68.39	73.06	77.72
		Avg. Cost \downarrow	0.36	5.00	0.16	0.50	<u>0.54</u>	3.46	2.81	4.93	1.03	0.85	0.79	0.89	1.11
	ChartQA	Avg. Acc. \uparrow	97.80	86.20	81.00	81.40	80.80	81.00	40.60	80.60	81.40	<u>83.00</u>	82.00	83.80	81.80
		Avg. Cost \downarrow	0.21	2.19	0.14	0.14	0.17	1.09	0.69	0.91	<u>0.16</u>	0.21	0.25	0.25	0.16
	DocVQA	Avg. Acc. \uparrow	98.56	91.48	78.95	78.66	80.48	85.55	82.30	81.44	<u>83.06</u>	80.48	79.52	82.58	79.04
		Avg. Cost \downarrow	0.18	2.18	0.14	0.15	0.18	1.22	1.25	0.74	0.36	0.20	0.21	0.29	<u>0.16</u>
All Datasets	OCRBench	Avg. Acc. \uparrow	99.06	89.20	80.28	77.00	81.22	<u>85.92</u>	79.34	78.40	83.10	84.04	83.57	87.32	79.34
		Avg. Cost \downarrow	0.23	2.41	0.14	0.16	0.19	1.44	0.96	0.78	0.28	0.20	0.22	0.32	<u>0.17</u>
	TextVQA	Avg. Acc. \uparrow	89.46	73.85	72.13	70.98	72.13	67.05	66.09	64.37	70.31	71.46	70.31	70.59	<u>72.13</u>
All Datasets		Avg. Cost \downarrow	0.18	2.15	0.13	<u>0.14</u>	0.16	1.12	1.81	0.39	0.20	0.17	0.15	0.25	0.13
	All Datasets	Avg. Acc. \uparrow	95.60	78.01	62.43	66.26	70.68	75.49	70.01	73.20	<u>73.31</u>	71.35	72.07	72.02	69.97
		Avg. Cost \downarrow	0.37	2.72	0.14	0.38	<u>0.41</u>	2.18	2.21	1.85	<u>0.52</u>	0.74	0.73	0.48	0.50
		Rank Score \uparrow	93.68	68.88	64.63	67.13	71.09	68.92	64.62	68.26	73.01	70.38	71.07	<u>72.01</u>	70.06

Table A4. Performance comparison of router methods on VL-RouterBench across datasets for $\lambda = 1000.0$. **Avg. Acc.** is average accuracy (%), **Avg. Cost** is average cost (\$/10K samples). The best and second-best results among learned routers are highlighted in **bold** and underlined, respectively (excluding Oracle and baseline methods).

Group	Dataset	Metric	Baselines			Hard Label				Soft Label ($\lambda = 1000.0$)					
			Oracle	Strongest	Cheapest	KNN	PRkNN	OVR	K-means	Linear	MLP	CosineCls	RouterDC	VLC	ZOOTER
General	HallusionBench	Avg. Acc. \uparrow	99.46	71.89	57.84	40.54	43.24	66.49	70.27	68.11	46.49	57.84	56.22	57.30	57.30
		Avg. Cost \downarrow	0.23	2.97	0.14	0.18	0.21	1.67	2.89	1.62	0.18	0.14	0.20	<u>0.14</u>	0.14
	InfoVQA	Avg. Acc. \uparrow	96.49	83.28	53.68	58.36	61.87	<u>81.10</u>	80.60	81.27	59.36	55.18	65.05	54.01	53.68
		Avg. Cost \downarrow	0.37	2.19	0.14	0.24	0.29	1.49	2.09	1.17	0.22	0.16	0.45	<u>0.15</u>	0.14
	MMBench	Avg. Acc. \uparrow	98.16	89.86	69.59	69.59	<u>81.11</u>	85.25	70.97	80.18	76.96	73.27	77.88	72.35	70.97
		Avg. Cost \downarrow	0.24	2.22	0.13	0.19	0.27	2.26	1.17	1.43	0.21	0.19	0.23	<u>0.17</u>	0.13
STEM	MMMU	Avg. Acc. \uparrow	98.46	74.36	45.64	42.05	53.33	60.00	65.64	<u>61.03</u>	47.69	49.74	54.36	45.13	43.08
		Avg. Cost \downarrow	0.64	3.24	0.17	0.41	0.43	6.95	10.59	4.69	0.26	0.33	0.52	<u>0.18</u>	0.17
	MMStar	Avg. Acc. \uparrow	96.68	72.76	49.17	54.48	59.80	68.44	<u>66.11</u>	64.45	54.82	51.50	57.81	49.50	49.17
		Avg. Cost \downarrow	0.36	2.29	0.14	0.25	0.29	2.85	1.68	1.79	0.22	0.19	0.32	<u>0.15</u>	0.14
	RealWorldQA	Avg. Acc. \uparrow	99.32	77.40	67.12	55.48	63.70	67.81	60.27	65.75	61.64	<u>67.12</u>	65.07	65.75	67.12
		Avg. Cost \downarrow	0.22	2.20	0.13	0.14	0.18	1.46	1.17	1.06	0.14	0.14	0.28	0.13	<u>0.13</u>
Chart & Doc	AI2D	Avg. Acc. \uparrow	99.69	88.21	72.33	67.45	73.58	80.66	<u>76.42</u>	76.10	71.86	72.33	75.31	72.96	72.01
		Avg. Cost \downarrow	0.24	2.19	0.13	0.16	0.19	2.05	2.56	1.51	0.15	0.14	0.24	0.13	<u>0.13</u>
	MathVerse	Avg. Acc. \uparrow	90.36	49.74	23.05	59.77	<u>67.97</u>	68.75	66.93	66.93	56.90	60.29	64.19	40.89	23.05
		Avg. Cost \downarrow	1.06	4.67	0.18	1.64	1.70	4.01	3.19	3.19	1.35	1.37	3.75	<u>0.85</u>	0.18
	MathVision	Avg. Acc. \uparrow	89.55	38.81	13.43	28.36	23.88	35.82	46.27	<u>47.76</u>	31.34	52.24	43.28	31.34	13.43
		Avg. Cost \downarrow	1.77	8.16	0.17	1.23	<u>0.72</u>	13.10	5.64	5.56	1.03	1.78	1.47	1.01	0.17
Average	MathVista	Avg. Acc. \uparrow	95.85	75.13	51.30	53.89	70.98	77.20	<u>73.58</u>	72.02	56.99	67.88	62.18	54.92	51.30
		Avg. Cost \downarrow	0.36	5.00	0.16	0.50	0.54	3.46	2.81	2.75	0.37	0.80	0.52	<u>0.28</u>	0.16
	ChartQA	Avg. Acc. \uparrow	97.80	86.20	81.00	81.40	80.80	81.00	40.60	80.20	81.40	<u>81.60</u>	84.20	81.00	81.00
		Avg. Cost \downarrow	0.21	2.19	0.14	0.14	0.17	1.09	0.69	0.60	0.18	0.15	0.24	<u>0.14</u>	0.14
	DocVQA	Avg. Acc. \uparrow	98.56	91.48	78.95	78.66	80.48	85.55	<u>82.30</u>	81.05	79.43	78.95	80.67	79.23	78.85
		Avg. Cost \downarrow	0.18	2.18	0.14	0.15	0.18	1.22	1.25	0.70	0.15	0.14	0.22	<u>0.14</u>	0.14
All Datasets	OCRBench	Avg. Acc. \uparrow	99.06	89.20	80.28	77.00	81.22	85.92	79.34	80.75	80.75	80.75	<u>83.57</u>	80.75	80.28
		Avg. Cost \downarrow	0.23	2.41	0.14	0.16	0.19	1.44	0.96	0.79	0.20	0.15	0.19	0.14	<u>0.14</u>
	TextVQA	Avg. Acc. \uparrow	89.46	73.85	72.13	70.98	<u>72.13</u>	67.05	66.09	66.95	71.65	72.13	71.55	72.22	72.13
All Datasets		Avg. Cost \downarrow	0.18	2.15	0.13	0.14	0.16	1.12	1.81	1.14	0.14	0.13	0.16	<u>0.13</u>	0.13
	All Datasets	Avg. Acc. \uparrow	95.60	78.01	62.43	66.26	70.68	75.49	70.01	<u>73.40</u>	67.75	68.65	71.17	65.21	62.33
		Avg. Cost \downarrow	0.37	2.72	0.14	0.38	0.41	2.18	2.21	1.57	0.33	0.35	0.72	<u>0.24</u>	0.14
		Rank Score \uparrow	93.68	68.88	64.63	67.13	71.09	<u>68.92</u>	64.62	69.29	68.73	69.53	<u>70.31</u>	66.78	64.54

Table A5. Performance comparison of router methods on VL-RouterBench across datasets for $\lambda = 10000.0$. **Avg. Acc.** is average accuracy (%), **Avg. Cost** is average cost (\$/10K samples). The best and second-best results among learned routers are highlighted in **bold** and underlined, respectively (excluding Oracle and baseline methods).

Group	Dataset	Metric	Baselines			Hard Label				Soft Label ($\lambda = 10000.0$)					
			Oracle	Strongest	Cheapest	KNN	PRkNN	OVR	K-means	Linear	MLP	CosineCls	RouterDC	VLC	ZOOTER
General	HallusionBench	Avg. Acc. \uparrow	99.46	71.89	57.84	40.54	43.24	<u>66.49</u>	70.27	62.70	48.11	51.89	58.38	41.62	56.76
		Avg. Cost \downarrow	0.23	2.97	0.14	0.18	0.21	1.67	2.89	0.77	0.14	0.30	0.17	0.16	<u>0.14</u>
	InfoVQA	Avg. Acc. \uparrow	96.49	83.28	53.68	58.36	61.87	81.10	<u>80.60</u>	79.10	58.19	62.54	61.71	60.87	53.68
		Avg. Cost \downarrow	0.37	2.19	0.14	0.24	0.29	1.49	2.09	0.80	<u>0.20</u>	0.46	0.33	0.29	0.14
	MMBench	Avg. Acc. \uparrow	98.16	89.86	69.59	69.59	81.11	85.25	70.97	71.43	74.19	76.50	<u>82.03</u>	77.42	69.59
		Avg. Cost \downarrow	0.24	2.22	0.13	0.19	0.27	2.26	1.17	0.43	<u>0.16</u>	0.61	0.47	0.19	0.13
STEM	MMMU	Avg. Acc. \uparrow	98.46	74.36	45.64	42.05	53.33	<u>60.00</u>	65.64	55.38	44.10	53.33	45.13	44.10	45.13
		Avg. Cost \downarrow	0.64	3.24	0.17	0.41	0.43	6.95	10.59	1.20	<u>0.28</u>	8.07	6.11	0.30	0.17
	MMStar	Avg. Acc. \uparrow	96.68	72.76	49.17	54.48	59.80	68.44	<u>66.11</u>	51.83	53.82	60.13	55.81	54.82	49.17
		Avg. Cost \downarrow	0.36	2.29	0.14	0.25	0.29	2.85	1.68	0.49	<u>0.18</u>	3.12	1.77	0.20	0.14
	RealWorldQA	Avg. Acc. \uparrow	99.32	77.40	67.12	55.48	63.70	67.81	60.27	60.96	65.75	59.59	62.33	62.33	<u>67.12</u>
		Avg. Cost \downarrow	0.22	2.20	0.13	0.14	0.18	1.46	1.17	0.46	0.13	0.51	0.19	0.16	<u>0.13</u>
Chart & Doc	AI2D	Avg. Acc. \uparrow	99.69	88.21	72.33	67.45	73.58	80.66	<u>76.42</u>	70.44	70.91	73.58	73.43	72.17	72.33
		Avg. Cost \downarrow	0.24	2.19	0.13	0.16	0.19	2.05	2.56	0.51	<u>0.14</u>	0.38	0.27	0.15	0.13
	MathVerse	Avg. Acc. \uparrow	90.36	49.74	23.05	59.77	<u>67.97</u>	68.75	66.93	53.39	52.47	45.83	50.39	43.36	23.05
		Avg. Cost \downarrow	1.06	4.67	0.18	1.64	1.70	4.01	3.19	1.56	1.73	9.42	7.30	<u>0.79</u>	0.18
	MathVision	Avg. Acc. \uparrow	89.55	38.81	13.43	28.36	23.88	<u>35.82</u>	46.27	34.33	31.34	23.88	22.39	22.39	13.43
		Avg. Cost \downarrow	1.77	8.16	0.17	1.23	<u>0.72</u>	13.10	5.64	1.48	1.48	40.17	40.70	0.98	0.17
Average	MathVista	Avg. Acc. \uparrow	95.85	75.13	51.30	53.89	70.98	77.20	<u>73.58</u>	63.21	55.44	55.96	59.07	54.92	51.30
		Avg. Cost \downarrow	0.36	5.00	0.16	0.50	0.54	3.46	2.81	1.00	0.38	6.74	3.64	<u>0.31</u>	0.16
	ChartQA	Avg. Acc. \uparrow	97.80	86.20	81.00	<u>81.40</u>	80.80	81.00	40.60	76.60	81.40	81.40	83.00	81.20	81.00
		Avg. Cost \downarrow	0.21	2.19	0.14	0.14	0.17	1.09	0.69	0.33	0.15	0.24	0.22	0.17	<u>0.14</u>
	DocVQA	Avg. Acc. \uparrow	98.56	91.48	78.95	78.66	80.48	85.55	<u>82.30</u>	80.10	78.56	79.90	79.71	78.95	78.85
		Avg. Cost \downarrow	0.18	2.18	0.14	0.15	0.18	1.22	1.25	0.61	0.14	0.19	0.18	0.16	<u>0.14</u>
All Datasets	OCRBench	Avg. Acc. \uparrow	99.06	89.20	80.28	77.00	81.22	85.92	79.34	80.28	79.34	83.10	<u>83.57</u>	81.69	80.28
		Avg. Cost \downarrow	0.23	2.41	0.14	<u>0.16</u>	0.19	1.44	0.96	0.50	0.17	0.22	0.21	0.16	0.14
	TextVQA	Avg. Acc. \uparrow	89.46	73.85	72.13	70.98	72.13	67.05	66.09	66.67	71.55	70.11	<u>70.59</u>	69.92	<u>72.13</u>
All Datasets		Avg. Cost \downarrow	0.18	2.15	0.13	0.14	0.16	1.12	1.81	0.43	0.13	0.27	0.17	0.14	<u>0.13</u>
		Avg. Acc. \uparrow	95.60	78.01	62.43	66.26	<u>70.68</u>	75.49	70.01	68.55	66.60	76.17	76.91	65.47	62.36
		Avg. Cost \downarrow	0.37	2.72	0.14	0.38	0.41	2.18	2.21	0.71	0.38	2.48	1.93	<u>0.27</u>	0.14
All Datasets		Rank Score \uparrow	93.68	68.88	64.63	67.13	71.09	<u>68.92</u>	64.62	68.01	67.48	68.41	70.86	66.90	64.57

Table A6. Performance comparison of router methods on VL-RouterBench across datasets for $\lambda = \infty$. **Avg. Acc.** is average accuracy (%), **Avg. Cost** is average cost (\$/10K samples). The best and second-best results among learned routers are highlighted in **bold** and underlined, respectively (excluding Oracle and baseline methods).

Group	Dataset	Metric	Baselines			Hard Label				Soft Label ($\lambda = \infty$)					
			Oracle	Strongest	Cheapest	KNN	PRkNN	OVR	K-means	Linear	MLP	CosineCls	RouterDC	VLC	ZOOTER
General	HallusionBench	Avg. Acc. \uparrow	99.46	71.89	57.84	40.54	43.24	66.49	70.27	57.84	47.57	<u>78.38</u>	80.00	45.41	49.73
		Avg. Cost \downarrow	0.23	2.97	0.14	0.18	0.21	1.67	2.89	0.14	0.16	5.18	4.66	0.15	<u>0.14</u>
	InfoVQA	Avg. Acc. \uparrow	96.49	83.28	53.68	58.36	61.87	81.10	80.60	51.17	58.03	<u>81.77</u>	81.94	59.20	52.34
		Avg. Cost \downarrow	0.37	2.19	0.14	0.24	0.29	1.49	2.09	0.14	0.23	1.34	1.47	0.26	<u>0.14</u>
	MMBench	Avg. Acc. \uparrow	98.16	89.86	69.59	69.59	81.11	85.25	70.97	62.67	69.59	90.32	<u>90.32</u>	67.74	64.52
		Avg. Cost \downarrow	0.24	2.22	0.13	0.19	0.27	2.26	1.17	<u>0.15</u>	0.16	5.49	5.49	0.17	0.14
STEM	MMMU	Avg. Acc. \uparrow	98.46	74.36	45.64	42.05	53.33	60.00	65.64	37.95	39.49	<u>76.92</u>	77.44	41.03	37.44
		Avg. Cost \downarrow	0.64	3.24	0.17	0.41	0.43	6.95	10.59	<u>0.19</u>	0.28	17.30	17.60	0.24	0.17
	MMStar	Avg. Acc. \uparrow	96.68	72.76	49.17	54.48	59.80	68.44	66.11	46.51	55.15	<u>73.42</u>	74.09	51.16	46.84
		Avg. Cost \downarrow	0.36	2.29	0.14	0.25	0.29	2.85	1.68	0.20	0.20	8.08	7.93	<u>0.17</u>	0.15
	RealWorldQA	Avg. Acc. \uparrow	99.32	77.40	67.12	55.48	63.70	67.81	60.27	57.53	60.27	78.08	<u>75.34</u>	59.59	62.33
		Avg. Cost \downarrow	0.22	2.20	0.13	0.14	0.18	1.46	1.17	0.13	0.14	3.42	3.53	0.14	<u>0.13</u>
Chart & Doc	AI2D	Avg. Acc. \uparrow	99.69	88.21	72.33	67.45	73.58	80.66	76.42	66.20	67.30	87.11	<u>86.95</u>	68.08	67.45
		Avg. Cost \downarrow	0.24	2.19	0.13	0.16	0.19	2.05	2.56	0.13	0.14	7.02	7.09	0.14	<u>0.13</u>
	MathVerse	Avg. Acc. \uparrow	90.36	49.74	23.05	59.77	<u>67.97</u>	68.75	66.93	46.22	56.25	65.62	64.19	43.49	25.13
		Avg. Cost \downarrow	1.06	4.67	0.18	1.64	1.70	4.01	3.19	1.03	1.35	7.56	6.75	<u>0.96</u>	0.28
	MathVision	Avg. Acc. \uparrow	89.55	38.81	13.43	28.36	23.88	35.82	46.27	31.34	29.85	61.19	<u>61.19</u>	22.39	22.39
		Avg. Cost \downarrow	1.77	8.16	0.17	1.23	<u>0.72</u>	13.10	5.64	1.00	1.04	26.73	26.73	0.84	0.54
Average	MathVista	Avg. Acc. \uparrow	95.85	75.13	51.30	53.89	70.98	77.20	73.58	57.51	55.44	<u>77.20</u>	77.20	49.22	50.78
		Avg. Cost \downarrow	0.36	5.00	0.16	0.50	0.54	3.46	2.81	0.67	0.42	9.63	9.63	<u>0.30</u>	0.19
	ChartQA	Avg. Acc. \uparrow	97.80	86.20	81.00	81.40	80.80	<u>81.00</u>	40.60	80.00	80.00	79.20	80.60	80.40	80.60
		Avg. Cost \downarrow	0.21	2.19	0.14	0.14	0.17	1.09	0.69	0.16	0.16	2.08	2.04	0.16	<u>0.14</u>
	DocVQA	Avg. Acc. \uparrow	98.56	91.48	78.95	78.66	80.48	85.55	82.30	75.50	78.47	88.23	89.76	78.76	77.61
		Avg. Cost \downarrow	0.18	2.18	0.14	0.15	0.18	1.22	1.25	0.14	0.15	1.12	1.29	0.16	<u>0.14</u>
All Datasets	OCRBench	Avg. Acc. \uparrow	99.06	89.20	80.28	77.00	81.22	85.92	79.34	75.59	75.12	92.49	<u>92.49</u>	77.00	76.53
		Avg. Cost \downarrow	0.23	2.41	0.14	0.16	0.19	1.44	0.96	<u>0.15</u>	0.17	1.58	1.68	0.15	0.14
	TextVQA	Avg. Acc. \uparrow	89.46	73.85	72.13	70.98	72.13	67.05	66.09	70.69	<u>71.17</u>	68.58	68.68	69.83	69.83
All Datasets		Avg. Cost \downarrow	0.18	2.15	0.13	0.14	0.16	1.12	1.81	0.13	<u>0.13</u>	1.66	1.81	0.14	0.13
		Avg. Acc. \uparrow	95.60	<u>78.01</u>	62.43	66.26	70.68	75.49	70.01	62.92	65.93	77.49	78.23	63.87	60.43
		Avg. Cost \downarrow	0.37	2.72	0.14	0.38	0.41	2.18	2.21	0.28	0.33	3.49	3.46	<u>0.28</u>	0.16
All Datasets		Rank Score \uparrow	93.68	68.88	64.63	67.13	71.09	<u>68.92</u>	64.62	64.41	67.04	65.61	66.56	65.33	62.58